

Computer Simulation in Lignocellulosic Biomass Conversion Processes: A Review

Yi Kong,^a and Shiyu Fu^{a,b,*}

Much attention has been paid to the solubilization and conversion processes of cellulose, hemicellulose, and lignin to produce high value-added chemicals and fuels. Computer simulation shows great potential in understanding the conversion process of plant biomass. This paper reviewed the solubilization processes, catalytic conversion, and pyrolysis of cellulose, hemicellulose, and lignin by density functional theory and molecular dynamics. The authors also provide prospects for the challenges and future developments in this area.

DOI: 10.15376/biores.17.4.Kong

Keywords: Lignocellulosic biomass; Density functional theory; Molecular dynamics; Biomass conversion

Contact information: a: State Key Laboratory of Pulp and Paper Engineering, South China University of Technology, Guangzhou 510640, PR China; b: South China University of Technology-Zhuhai Institute of Modern Industrial Innovation, Zhuhai 519175, PR China; *Corresponding author: shyfu@scut.edu.cn

INTRODUCTION

With the continuous consumption of fossil fuels and consequent environmental problems, there is an urgent need for a green, renewable energy source. Biomass, also known as lignocellulosic biomass, is a widely renewable bioenergy source considered a potential alternative to conventional energy sources to alleviate human energy shortages and environmental problems (Xu *et al.* 2019). Lignocellulosic biomass is derived from numerous species, such as trees (pine, poplar, and eucalyptus), crops (corn, wheat, and rice), grasses, and its main components are usually cellulose, hemicellulose, and lignin (Zakzeski *et al.* 2010; Zhou *et al.* 2014, 2015). Figure 1 depicts the composition of lignocellulosic biomass from different sources (Xu *et al.* 2020a).

Agriculture-based biomass materials could be applied in wide areas. It is a hot topic that biomass is converted into liquid biofuels and chemicals. The conversion processes of biomass, including catalytic depolymerization, oxidation, hydrogenation, pyrolysis, and dissolution, involve complex chemical reactions and to some extent, lack of insight into the conversion mechanism. The limitations of traditional experimental methods in studying plant biomass conversion have made computer simulations a promising tool. Computer simulations can identify the best complex transformation pathways of plant biomass and understand the transformation mechanisms at the molecular and atomic levels (Buehler and Ackbarow 2007). In addition, computer simulations allow experiments to be inexpensively guided by models. For instance, computer simulations can help gain insight into the dissolution mechanisms of existing solvents, providing a basis for designing solvents with high selectivity and high dissolution efficiency. Similarly, computer simulations are applied to selecting catalysts in the catalytic conversion of biomass and the relationship between temperature and product in the pyrolysis process.

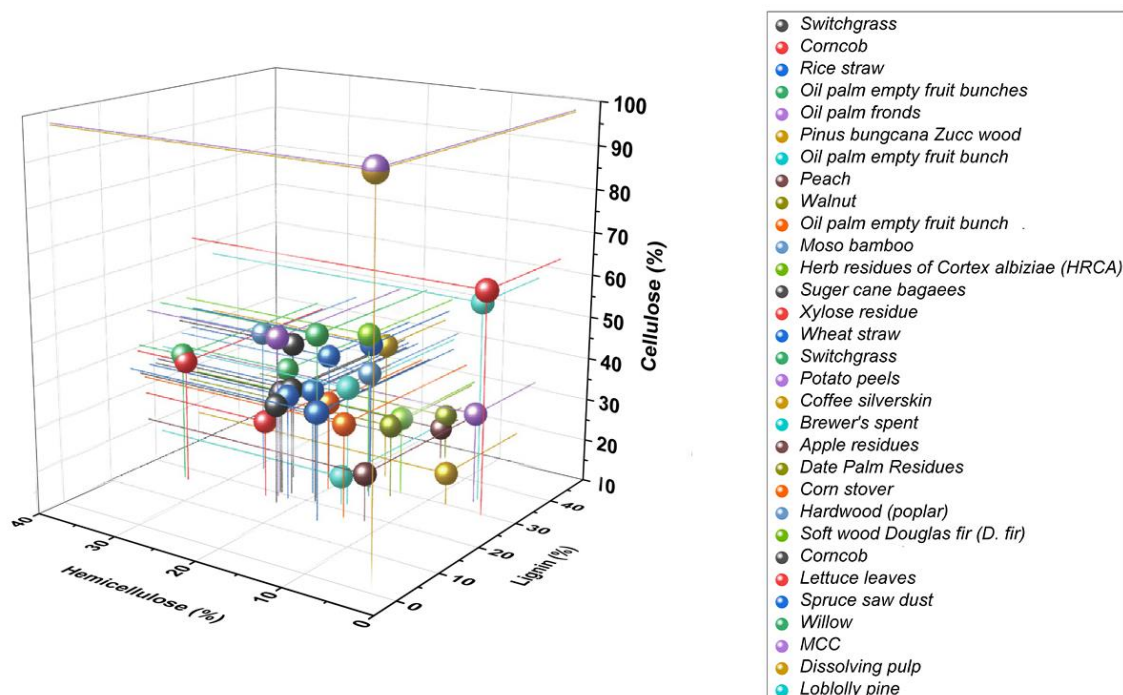


Fig. 1. Composition of biomass raw materials (Xu *et al.* 2020a; Reprinted with permission from Elsevier)

There is a conflict between the model's accuracy and the computational time in the simulation calculation. A high-precision model matching the actual situation requires more computation power or computation time. At the same time, these methods result in errors by simplifying the model or using more approximations. Two common computational methods, Density Functional Theory (DFT) and Molecular Dynamics (MD), have gained widespread attention in converting components of plant biomass (Sangha *et al.* 2012).

To improve the understanding of biomass conversion, this paper focuses on the conversion pathways and mechanisms of solubilization, catalytic conversion, and pyrolysis processes among cellulose, hemicellulose, and lignin using MD and DFT methods, including the structure of lignocellulosic materials, computational methods, and biomass conversion processes, which may provide a theoretical basis for the study of plant biomass. Finally, the challenges and future developments in biomass conversion are presented. Computational models and chemicals involved in this paper are organized in Table 1 in the order of appearance.

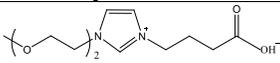
LIGNOCELLULOSIC MATERIAL COMPONENTS

Cellulose

Cellulose is the main component of lignocellulosic biomass and the most distributed and abundant homopolysaccharide in nature (Mood *et al.* 2013). Its molecule consists of glucose monomers linked by $\beta(1-4)$ bonds, and the adjacent glucose monomers are alternately rotated by 180° . The cellulose chains are arranged to form elementary fibrils with a diameter of about 3 to 4 nm, while the crystalline and non-crystalline regions of cellulose are present in the elementary fibrils. Elementary fibrils are further organized into

microfibrils with a diameter of 10 to 20 nm. At the same time, microfibrils, together with the surrounding matrix, such as hemicellulose and lignin, are combined to form macrofibril of the cell wall. (Gibson 2012).

Table 1. Names and Abbreviations of Computational Models and Chemicals

Chemicals		Models/Products	
Name/Structure	Abb.	Name	Abb.
N,N-dimethylacetamide	DMA	Veratrylglycerol- β -guaiacyl ether	VG
N-Methylmorpholine-N-oxide	NMMO	Levoglucosan precursor	pre-LGA
1-Butyl-3-methylimidazolium	[Bmim]	5-Hydroxymethylfurfural	HMF
1-Ethyl-3-methylimidazolium	[Emim]	Hydroxyacetaldehyde	HAA
Alkyl phosphate anion	(MeO) $_2$ PO $_2^-$	Pyruvaldehyde	PA
Tetrafluoroborate anion	BF $_4^-$	Furfural	FF
Hexafluorophosphate	PF $_6^-$	Phenethyl phenyl ether	PPE
Thiocyanate	SCN $^-$	Lactic acid	LaA
1-Octyl-3-methylimidazolium	[C $_8$ mim]	Dihydroxyacetone	DHA
	OE $_2$ imC $_3$ C	Levulinic acid	LA
Dimethyl sulfoxide	DMSO	Guaiacyl glycerol- β -guaiacyl ether	GG
1,3-Dimethylimidazolium	[C $_1$ mim]	Methyl p-hydroxycinnamate	MPC
1-Allyl-3-methylimidazolium	[Amim]	Phenyl p-hydroxycinnamate	PPC
1-Butyl sulfonic acid-3-methylimidazolium chloride	[C $_4$ SO $_3$ Hmim]	2-Hydroxyethyl phenyl ether	HPE
Sulfonated poly(phenylene sulfide)	SPPS	Benzyl phenyl ether	BPE
1-H-3-methylimidazolium chloride	[Hmim]	Diphenyl ether	DPE
Carbonized melamine foam	CMF	Phenylcyclohexane	PC
Carbon nanotube	CNT	2-Phenoxy-1-phenylethanol	2-P-1-PE
		2-Phenoxyethanol	2-PE

The following types of cellulose are currently known: cellulose I, II, III, IV, and their sub-types. Naturally occurring cellulose is defined as cellulose I, which together with cellulose II are the most common and widely used cellulose models in computational simulations (O'Sullivan 1997). Figure 2 shows the 36-chain model of crystalline cellulose I β microfibril. The dense crystalline structure of the cellulose crystalline region provides the plant high mechanical strength, but severely hinders the access of chemical reagents and enzymes to the cellulose, leading to difficulties in the degradation of natural cellulose. Therefore, it is necessary to understand its structure-property and other important information to use cellulose materials better.

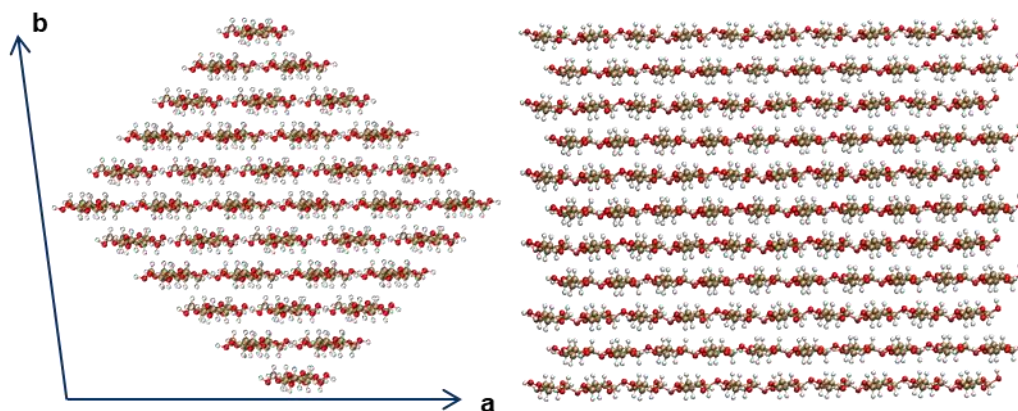


Fig. 2. A 36-chain 3D model of crystalline cellulose I β microfibril: a) View along the c direction; b) view along the b direction of the cellulose microfibril segment (10 glucopyranose units along the c direction). Tan: carbon atoms; red: oxygen atoms; white: hydrogen atoms.

Hemicellulose

Hemicellulose, another polysaccharide abundant in nature, is a homopolymer or heteropolymer composed of main and branched chains (Rivas *et al.* 2016). The type of monosaccharides, the type and location of chemical bonds, and the distribution of side chains of hemicellulose vary considerably with the source of biomass. The composition of hemicellulose and the monomer species after hydrolysis were described in detail by Girio and colleagues (Girio *et al.* 2010). Different monosaccharides are present in the short side chain branches of hemicellulose, including pentoses (xylose, rhamnose, and arabinose), hexoses (glucose, mannose, and galactose), and glyoxylates (glucuronides and galacturonic acids) (Terrett and Dupree 2019).

Typical representatives of hemicelluloses are glucomannan and xylan, the most abundant components in the secondary cell walls of herbs and hardwoods. Xylan is mainly chosen as a hemicellulose model in the simulation of biomass conversion processes while decorated with different side chains to meet various experimental objectives. The typical structure of hemicellulose substituted with acetate, ferulate, and glucuronide is shown in Fig. 3.

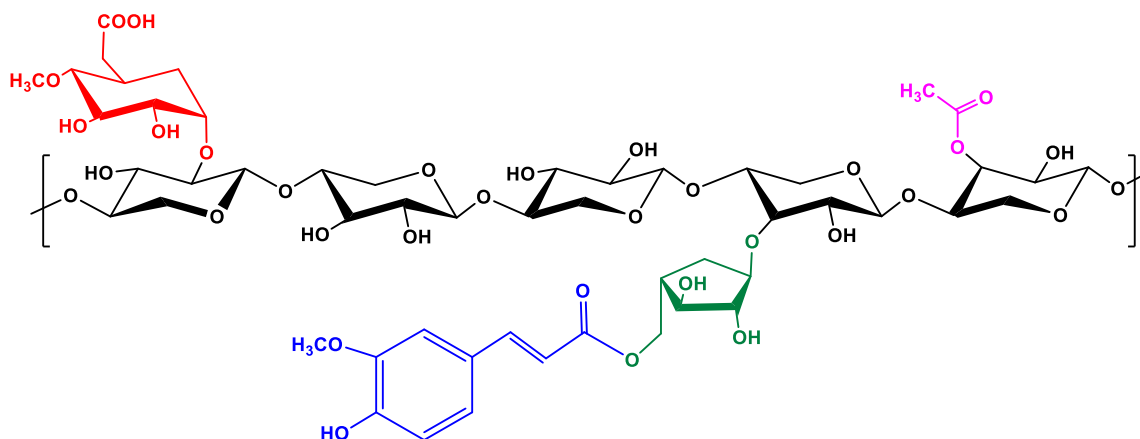


Fig. 3. Typical structure of hemicellulose substituted by acetyl (pink), arabian furan (green), ferulate (blue), and 4-O-methyl gluconic acid (red)

Lignin

Lignin is an amorphous and complex natural polymer. It plays a supporting role in plants and enhances mechanical strength and stiffness by binding to cellulose fibers. Lignin is composed of three basic structural units: the para-hydroxyphenyl lignin (H unit), the guaiacyl lignin (G unit), and the syringyl lignin (S unit). The content of each unit varies considerably among the different sources of lignin. For example, the major component of cork lignin is the G-unit with small amounts of S and H-units, while the lignin of deciduous trees contains approximately equal parts of S and G-units and less of H-units. The ratio of G: S: H in monocot grasses is about 70:25:5 (Feofilova and Mysyakina 2016). The major chemical bonds between these units are β -O-4, β -5, β - β , 5-5, 4-O-5, and β -1 (Garcia Calvo-Flores and Dobado 2010; Ralph *et al.* 2019). Lignin contains many functional groups, including methoxy, phenolic hydroxyl, aliphatic hydroxyl, carboxyl, and carbonyl groups. The presence of functional groups contributes to the extremely complex lignin structure. It gives the cell wall of plants the ability to resist attack by external environments (*e.g.*, enzymes, chemicals, and microorganisms) (Lancefield and Westwood 2015). The model structures of lignin are shown in Fig. 4.

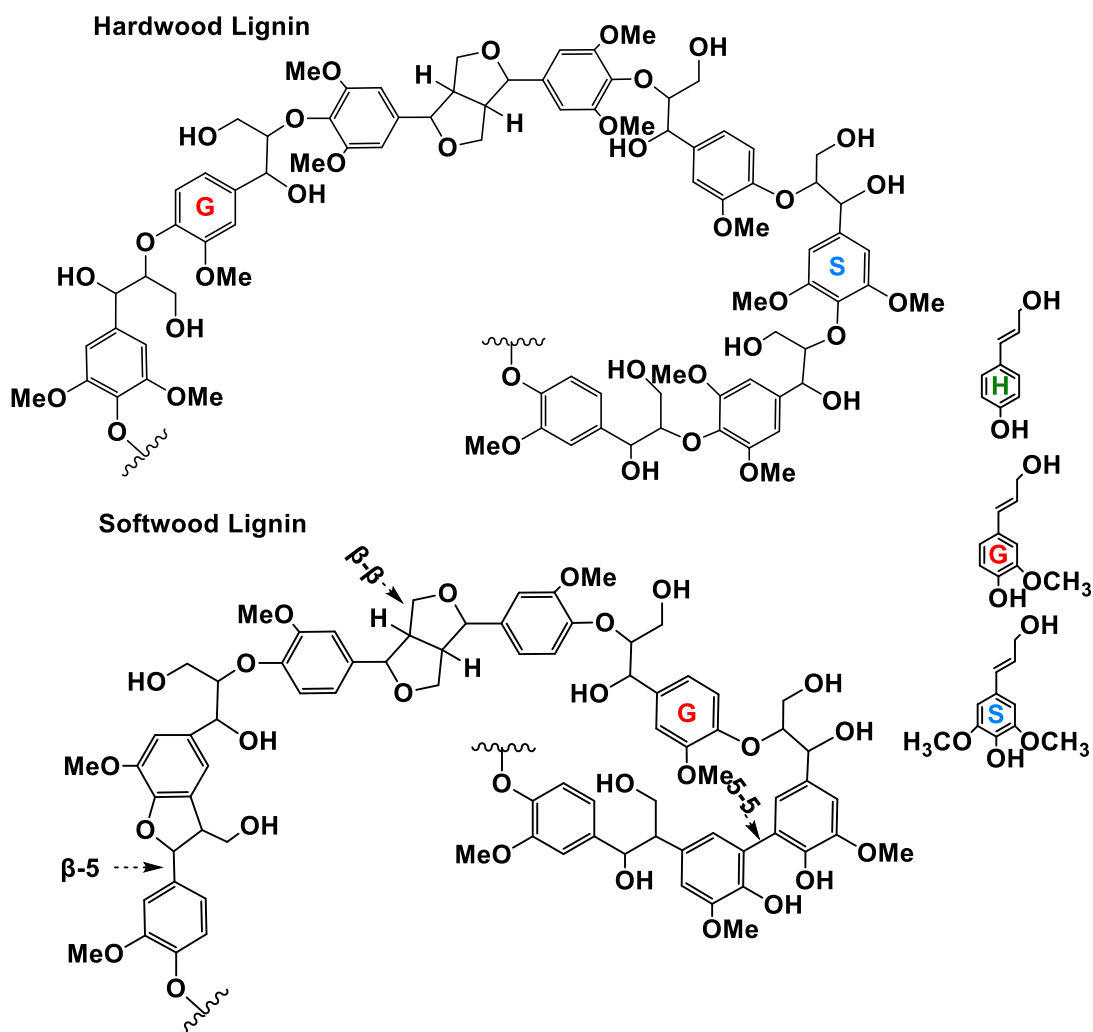


Fig. 4. Model structures of hardwood and softwood lignin (Lancefield and Westwood 2015; Reprinted under Creative Commons Attribution 3.0 from RSC)

COMPUTATIONAL SIMULATION METHODS

With the rapid development of computers, various theoretical computational methods emerged, involving computational models that can be built at multilength and time scales. The length scales can be scaled up to the atomic level and the macroscopic scale. Simulations are possible on time scales ranging from picoseconds (ps) to seconds (s) (Zhang *et al.* 2019c; Zhou *et al.* 2021). Among the many theoretical computational methods, DFT and MD methods are widely used by researchers because of their excellent performance in terms of conformity to experimental data (Petridis *et al.* 2011; Sangha *et al.* 2012).

DFT

The method DFT studies the electronic structure of multi-electron systems by electron density and is widely used in condensed matter physics, materials science, quantum chemistry, and life sciences (Grimme 2011). The basic concept of DFT is to reduce intractable problems (electron-electron interactions) to interaction-free issues through various approximations and to integrate all errors in one term for analysis (Thomas 1927). The method began with the Thomas-Fermi model (Thomas 1927), which introduced the concept of density generalization and simplified the computational form and process, but did not take into account the interaction between electrons and did not provide an accurate description of the kinetic energy term, and therefore was not applicable in many systems. Until the 1960s, the Hohenberg-Kohn theorem and the Kohn-Sham equation were proposed to improve the content of DFT and finally established a strictly meaningful density functional computational theory. (Hohenberg and Kohn 1964; Kohn and Sham 1965; Kim *et al.* 2013). The most widely used functionals in DFT are M06-2x, B3LYP, X3LYP, and B3PW91, among which the most widely used and popular functional in plant biomass conversion simulation is B3LYP (Qi *et al.* 2016). These functionals (PBE, PW91, BLYP, and B3LYP) are deficient in describing dispersion interactions and examining electrostatically dominated weak interactions such as hydrogen bonding (Grimme 2011). To address the problem, Grimme proposed the dispersion-corrected DFT functionals (DFT-D), which had four versions, namely DFT-D1 (Grimme 2004), D2 (Grimme 2006), D3 (Grimme *et al.* 2010), and D4 (Caldeweyher *et al.* 2017). Subsequently, Grimme demonstrated through an extensive test set that the DFT-D3 functional had an excellent performance in describing non-covalent interactions of non-polar moieties or neutral systems (Goerigk and Grimme 2011). The DFT-D3 version has high accuracy and a small increase in time consumption. Moreover, it has a high degree of fit in the adaptation of mainstream functionals and mainstream quantitative programs.

MD

Although DFT could accurately describe the relevant properties of electrons, it cannot deal with larger systems due to a large amount of computation required. The method MD was undoubtedly an excellent choice when dealing with complex biological systems. Through analyzing atoms and molecules as a whole particle to analyze their motions, while the details inside the particle are simplified or disregarded, thus greatly reducing the computational requirements of each particle, MD simulation is the most suitable choice to balance basic accuracy and computational efficiency (Dong *et al.* 2017; Zhou *et al.* 2021).

The MD can be used to calculate macroscopic properties of substances or systems, such as density, solubility, melting and boiling points, enthalpy of evaporation, dielectric

constant, and viscosity (Jung *et al.* 2018, 2019; Petridis *et al.* 2011). It is also used to view the microscopic properties, structure, and characteristics of a system, such as the spatial distribution of atoms or molecules, the trajectory of particles, the ratio of conformational distribution, diffusion dissolution, and adsorption processes (Yui and Hayashi 2007). The freedom of the studied system is very high. The simulation environment (temperature, pressure, external electric field, and external forces) could be set for the purpose, and all information inside the system is unambiguous. The range of systems studied by MD simulations is enormous, with common systems, such as proteins, nucleic acids, polysaccharides, polymers, metals, inorganic materials, and various small molecules, among others. The molecular force field, one of the important components of MD theory, is applied to describe the interaction potential between atoms. Common force fields include AMBER (Damm *et al.* 1997) (Assisted Model Building with Energy Refinement), GAFF (General AMBER Force Field), GLYCAM (Kirschner *et al.* 2008) (Glycans and Glycoconjugates in AMBER), OPLS (Damm *et al.* 1997) (Optimized Potentials for Liquid Simulations), GROMOS (Oostenbrink *et al.* 2004) (Groningen Molecular Simulation), CHARMM (Brooks *et al.* 1983) (Chemistry at Harvard Macromolecular Mechanics), CGenFF, COMPASS, GROMOS series (Hermans *et al.* 1984), PCFF, *etc.* In addition, chemical reaction processes could be simulated with ReaxFF (van Duin *et al.* 2001) (reaction force fields), called ReaxFF Reaction Molecular Dynamics (ReaxFF-RMD) (Xu *et al.* 2021a).

DISSOLUTION MECHANISM

Efficient, non-polluting dissolution systems are essential for the widespread use of plant biomass feedstocks. The screening of solvents by experimental methods is quite complicated, time-consuming, and costly. To better guide experiments and design solvents, researchers relied on computer simulations and modeling to gain insight into the dissolution mechanism. In this section, the dissolution processes and mechanisms of cellulose, hemicellulose, and lignin substrates are investigated by the MD method mainly and the DFT method as a supplement.

Cellulose Dissolution Mechanism

The interaction between cellulose and solvents is a hot topic of research on cellulose. Water can swell cellulose materials but not dissolve in water. Mazeau and Rivet used MD to simulate the wetting of cellulose (110) and (100) planes by water. The simulation results showed that the (100) plane dissolved more slowly than the (110) plane. The cellulose crystal structure of both planes remained unchanged (Mazeau and Rivet 2008). Bergensträhle and co-workers simulated the dissolution behavior of cellulose crystals in aqueous solutions. The results showed that both the accumulation of hydrophobic groups and the hydrogen bonding in the cellulose chains inhibited the dissolution of cellulose crystals (Bergensträhle *et al.* 2010). Similarly, Malaspina and Faraudo investigated the interaction of different molecules with the (100) and (010) planes of cellulose. The (100) and (010) planes are both hydrophilic and lipophilic, as indicated by the contact angles of water and tetradecane on the I β cellulose plane. The wetting of cellulose planes under water and organic solvent conditions is strongly heterogeneous on the molecular scale. Both hydrophilic and hydrophobic ions interacted weakly with the nanocellulose surface, although the interaction of the hydrophobic ions with the cellulose

surface seems to be stronger than that of the hydrophilic ions. This result could be attributed to the fact that the cellulose surface had both hydrophilic and lipophilic behavior. (Malaspina and Faraudo 2019). Gross and co-workers simulated the dissolution of cellulose in four solvents, LiCl/ N,N-dimethylacetamide (DMA), water, LiCl/water, and DMA. It was found that LiCl/DMA had the best solubility for dextran chains. Due to the low solubility of dextran and LiCl in DMA, Li⁺ and Cl⁻ could effectively interact with glucose, resulting in the dissolution of cellulose. The small size of the cation preferentially interacts strongly with cellulose, which is considered the main driving force responsible for cellulose dissolution (Gross *et al.* 2013).

In addition, solvents, such as aqueous sodium hydroxide (Miyamoto *et al.* 2015), sodium hydroxide/urea system (Liu *et al.* 2018), N-Methylmorpholine-N-Oxide (NMMO) (Rabideau and Ismail 2015), and ionic liquids (ILs) (Li *et al.* 2015b; Yuan and Cheng 2015; Li *et al.* 2017b), are used to dissolve cellulose. Cellulose solubilization in aqueous sodium hydroxide solution is almost unrelated to the direct interaction of OH⁻ with cellulose. Water molecules and Na⁺ can penetrate cellulose crystals from the interlayer space in the (1-10) plane, so that hydrophobic sheets are dissociated into microcrystals, which then become independent chains (Miyamoto *et al.* 2015). Wang and co-workers investigated the dissolution process of cellulose in aqueous solutions of five quaternary ammonium hydroxides and found that the hydrophobicity of cations was the main driving force for cellulose dissolution. The hydrophobic cations aggregated at the cellulose interface, reducing the surface tension and facilitating cellulose dispersion (Wang *et al.* 2018).

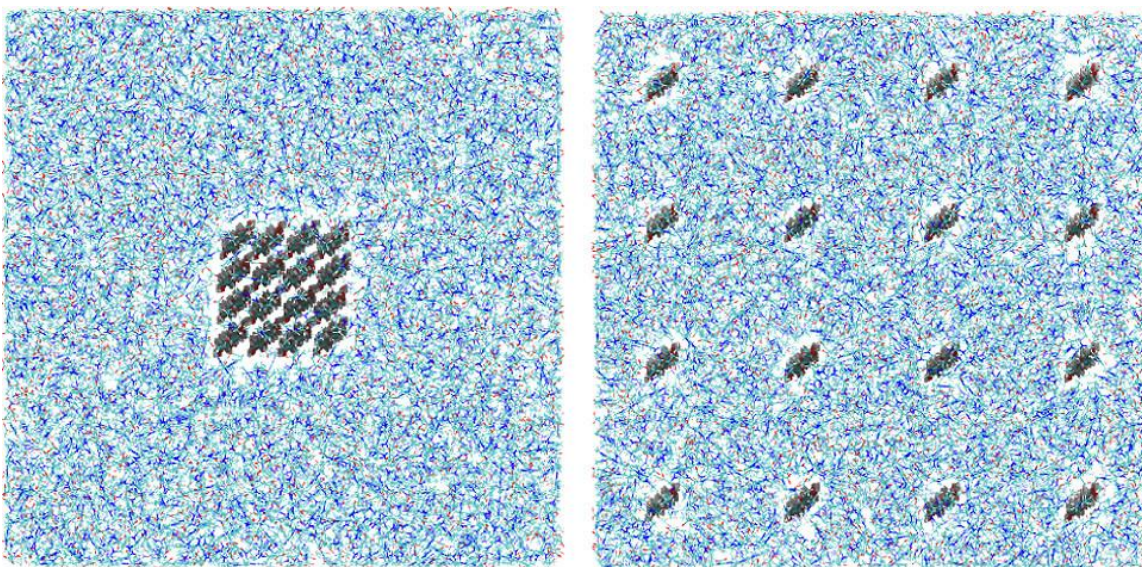


Fig. 5. Crystalline and dissociated states of the 15 wt% cellulose solution. Reprinted with permission from (Rabideau and Ismail 2015). Copyright 2015 American Chemical Society.

Using MD, cellulose dissolution was investigated in aqueous NaOH/urea solutions, and showed that the cellulose inclusion complex was anisotropic. In this system, Na⁺ and OH⁻ are located in the hydroxyl and hydroxymethyl regions of the cellulose molecule, and the urea molecule occupies the surface of the hydrophobic pyranose ring (Liu *et al.* 2018). The role of urea dissolving cellulose is that it preferentially absorbs the hydrophobic surface of the glucose ring and gradually weakens the hydrophobic effect of the cellulose chain (Wernersson *et al.* 2015). The NMMO was also a good solvent for solubilizing

cellulose. Rabideau and Ismail constructed the model shown in Fig. 5 and found that cellulose dissolved spontaneously when the ratio of NMMO to water was close to 1:1. The formation of NMMO-cellulose and water-cellulose hydrogen bonds promote the dissolution of cellulose (Rabideau and Ismail 2015).

Recently, the dissolution of lignocellulosic materials (especially cellulose) in IL is excellent, but the dissolution mechanism of IL is still not perfect. In 2007, Liu and co-workers performed MD calculations for cellobiose/[Bmim]Cl at different temperatures. The anion was closer to the cellobiose than the cation, and the moderate to strong hydrogen bonds formed the anion with the hydroxyl groups of the cellobiose in a ratio close to 1:1. The imidazole cation is involved in the π - π stacking interaction (Liu *et al.* 2007). Yao and co-workers also applied cellobiose as a model and investigated the solubilization mechanism of cellulose in [Bmim]Cl, [Emim]Cl, and [Emim]OAc by the DFT method. They indicated that anions played an essential role in the reaction process while cations had little influence (Yao *et al.* 2015).

A MD simulation of cellulose distribution in [Bmim]Cl using 36 cellulose chains with a degree of polymerization of 16 showed that the anions tended to form hydrogen bonds with glucose, while the cations were closer to the cellulose chains in the axial direction (Gross *et al.* 2011). The interaction of cellulose molecules was investigated with several of the most common anions in imidazolyl ILs by DFT calculations. The anion forming hydrogen bonds with hydroxyl protons of cellulose is a key factor in solubilizing cellulose. The strength of the anion interactions with cellulose was in the following order: $\text{Cl}^- > \text{OAc}^- > (\text{MeO})_2\text{PO}_2^- > \text{BF}_4^- > \text{PF}_6^-$, $\text{SCN}^- > \text{PF}_6^-$ (Guo *et al.* 2010; Zhao *et al.* 2013). The solubilization effect of 13 ILs with fixed anions (OAc^-) on cellulose showed that the acidic protons on the cationic heterocycles were necessary for cellulose solubilization, while the Van der Waals interactions between the cations and cellulose were not important. These cations with highly electronegative atoms in the main chain or large size groups in the alkyl chain would reduce cellulose solubility (Lu *et al.* 2014). The ILs were diverse and easy to design, and after the initial understanding of the mechanism of cellulose solubilization by ILs, researchers placed more attention on developing and designing efficient ILs.

Steric hindrance is the key to developing a preferred solvent for cellulose. The volume and flexibility of the cationic structure must be considered while maintaining the anionic polarity. Two ILs, [C₈mim]OAc and OE₂imC₃C, were able to solubilize cellulose but not xylan within 60 min. The MD calculations showed that the polysaccharide formed a stable hydrogen bonding network in [Emim]OAc, but a relatively unstable hydrogen bonding structure in OE₂imC₃C. [Emim]OAc and OE₂imC₃C had similar hydrogen-bonding networks, and the difference in the ability to solubilize cellulose and xylan might be attributed to spatial site resistance (Kadokawa *et al.* 2021). Meng and co-workers designed 20 ILs based on tetraalkylammonium cations and OAc^- for their ability to solubilize cellulose and found that the solubilization effect was highly dependent on the size of the ions, and the most effective ILs were less viscous (Meng *et al.* 2017).

Researchers found that ILs containing entraining agents could also solubilize cellulose, sometimes with better solubilization than pure IL systems. Dimethyl sulfoxide as an auxiliary reduced the viscosity of ionic liquids, thus improving the solventization of ionic liquids (Meng *et al.* 2017). The MD results indicate that DMSO does not interact specifically with glucose and would not significantly affect the specific interactions between cations and anions or between ionic liquids and polymers (Andanson *et al.* 2014; Velioglu *et al.* 2014). Compared to DMSO, water molecules might be closer to the glucose

ring, thus interfering with the IL-glucose interaction, which might be the reason for the unsuitability of water as a coagent in ILs of solubilized cellulose (Huo *et al.* 2013; Andanson *et al.* 2014). Due to this property of water, it could be used as a regenerative solvent for cellulose (Gupta *et al.* 2013). The MD further showed that the anti-solvent had a strong affinity for ILs, and the H-bond between cellulose and ILs was broken, promoting the regeneration of cellulose (Ju *et al.* 2022).

Hemicellulose Dissolution Mechanism

Few simulation studies were performed for the hemicellulose dissolution process and mechanism. The DFT method is applied to calculate the solubilization mechanism of hemicellulose and cellulose in solvents ([C₁mim]OAc, water, and methanol). It was found that the binding energy between xylan and IL was 20 kcal/mol stronger than that between cellulose and IL (Payal *et al.* 2012). Mohan and co-workers screened 1428 ILs by the COSMO-RS model. Subsequently, OAc⁻ and [Emim] are considered better candidate ions for solubilization of cellulose and hemicellulose by interaction energy calculations. The hydrogen bonding between the hydroxyl group and the anion of cellulose/hemicellulose was determined, the dissolution order of cellulose and hemicellulose in ionic liquids was tentatively determined, and the anion of IL was determined to play a dominant role in the dissolution process (Mohan *et al.* 2018). Moyer and co-workers studied the potential of ionic liquids to solubilize lignocellulosic biomass, and [Amim]formate proved to be the most effective, especially in solubilizing hemicellulose (Moyer *et al.* 2018).

Lignin Dissolution Mechanism

Lignin is a major natural source of aromatic compounds, but it is difficult to achieve high-value utilization from lignin because of its structural recalcitrance and complexity. Lignin is more soluble in organic solvents than cellulose, and lignin oligomers are even soluble in water. Three lignin-water systems were simulated by Vu and co-workers using the PCFF force field. The lignin models were decamers composed of only G, S, or H units connected only by β -O-4. The simulation results showed that the reduced mobility of water molecules in the hydroxyl and methoxy regions of lignin was due to the hydrogen bond formation and hydrophobic effects, respectively (Vu *et al.* 2002). The solubilization behavior of enzymatic lignin in different organic-water systems showed that enzymatic lignin dissolved in acetone-water mixtures with a volume ratio of 7:3, while aggregated in water, ethanol, acetone, and tetrahydrofuran. The hydrophobic backbone and hydrophilic groups of lignin were solvated by acetone and water molecules, respectively, leading to lignin solubilization. Conversely, only the hydrophobic backbone or the hydrophilic groups were solvated in organic solvent or water, respectively, inducing serious lignin aggregation (Wang *et al.* 2020).

Ionic liquids are good solvents not only for cellulose but also for lignin. The interaction of Veratrylglycerol- β -Guaiacyl ether (VG) with [Amim]Cl was studied with DFT and MD simulations. The VG monomer had strong intramolecular hydrogen bonding, and its dimer had π - π stacking and hydrogen bonding interactions. The anion of [Amim]Cl played a more important role in lignin solubilization than the cation (Zhu *et al.* 2017). A cork-like lignin polymer was modeled by Manna and co-workers using 61 G units as the starting structure. The MD simulations of lignin were performed in the [Emim]OAc-water solvent system. In 50% and 80% of [Emim]OAc, the lignin structure was significantly unstable, and the pure [Emim]OAc system disrupted the intra-chain hydrogen bonds. The anion interacted mainly with the alkyl chain and hydroxyl group of lignin. In addition, the

cationic imidazole group contributed to the solventization of the methoxy and hydroxyl groups, while the cationic ethyl group interacted with the benzene ring (Manna *et al.* 2021). Shi and co-workers used an [Emim]OAc-water mixture to study the pretreatment of switchgrass at 160 °C. The chemical composition and crystallinity of the pretreated biomass and the dissolution and depolymerization of lignin depended on the [Emim][OAc] concentration (Shi *et al.* 2014). Janesko conducted a comprehensive study to elucidate the non-covalent interactions between various ILs and cellulose/lignin. The ILs with π -conjugated cations favored the solubility of lignin (Janesko 2011).

PYROLYSIS MECHANISM

Pyrolysis is the thermal or thermochemical degradation of biomass materials under conditions of air isolation or supply of small amounts of air. It has become one of the common ways to utilize biomass. This section elucidates the pyrolysis mechanisms of cellulose, hemicellulose, and lignin at different temperatures by DFT and MD.

Cellulose Pyrolysis Mechanism

The reaction pathway of β -D-glucopyranose pyrolysis was investigated to synthesize gas (CO, H₂) using the DFT method. The involvement of reactive hydrogen atoms could lower the reaction energy barrier. The CO was mainly from the decomposition of aldehyde groups, and H₂ was mainly from the dehydrogenation process (Huang *et al.* 2013). Murillo and co-workers used MD to study the differences between maltose and cellobiose. The better thermal stability of fibrous disaccharides (gg and gt conformations) was attributed to the formation of stable intra- and inter-ring hydrogen-bonding networks (Murillo *et al.* 2015). In addition, the initial decomposition of cellulose pyrolysis was simulated at 600.15 K and 873.15 K using Car-Parrinello MD. The simulated cells and the main pyrolysis products are shown in Fig. 6. The pyrolysis products were mainly pre-LGA with by-products such as HMF and formic acid. At 873.15 K, the products' energy barriers were: pre-LGA < pre-HMF < formic acid, which could prove that LGA was the main product of the rapid pyrolysis of cellulose (Agarwal *et al.* 2012). Yang and co-workers investigated the formation mechanisms of the three most abundant cellulose pyrolysis components, LGA, HAA, and PA. The LGA was likely formed by a synergistic mechanism; HAA could be formed from C1-C2 and C5-C6 by ring-opening and dehydration reactions, while PA was formed by ring-opening reactions followed by dehydration and transaldol reactions. The formation of HAA and PA competes with the formation of LGA (Yang *et al.* 2020).

Cellulose pyrolysis at temperatures of 1000 to 3000 K using the ReaxFF-RMD method simulated the conversion pathways of seven major products and concluded that the C-O bond within the pyran ring was the most susceptible to breakage (Liu *et al.* 2021b). The effect of CaO on the pyrolysis of cellulose using ReaxFF-RMD simulations showed the addition of CaO significantly promoted the pyrolysis of cellulose and immobilized more oxygen-containing groups with the increase of Ca/C mass ratio by CaO. The total number of C-O bonds in the system after adding CaO was lower than in the pure cellulose pyrolysis system, and the number of CO and H₂O molecules was reduced (Si *et al.* 2019). When co-pyrolysis of cellulose and polyethylene was conducted, the hydrocarbon and H radicals from polyethylene interacted with the alcoholic groups and furans, which contributed to producing alcohols and suppressed the generation of aldehydes and ketones.

In the presence of polyethylene, hydrogenation reactions readily occurred, contributing to the production of furanol (Wang *et al.* 2021c).

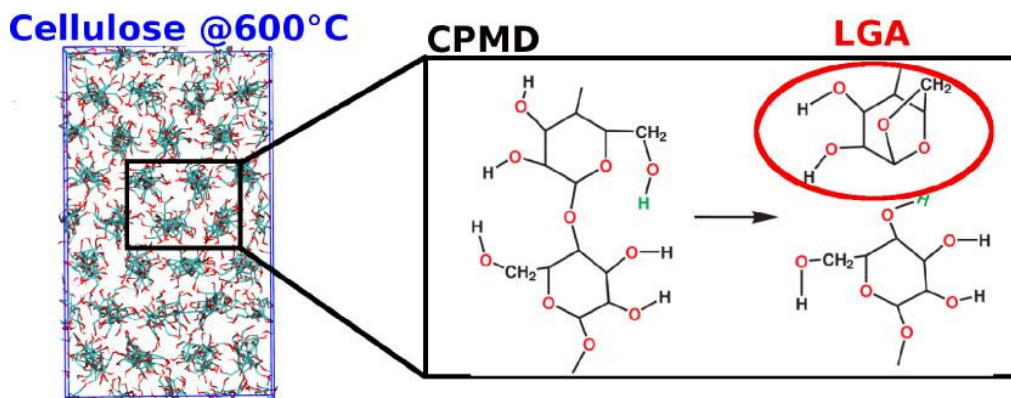


Fig. 6. Nascent decomposition processes in cellulose pyrolysis. Reprinted with permission from (Agarwal *et al.* 2012). Copyright 2012 American Chemical Society.

Hemicellulose Pyrolysis Mechanism

Due to the complex composition and branching structure of hemicelluloses, initial simulation studies of hemicellulose pyrolysis mechanisms usually used monosaccharides or disaccharides as models. The pyrolysis processes of xylose and arabinose under the M06-2X/6-31++G(d,p) level using the DFT method indicated that there were eight possible pyrolysis pathways for xylose and five for arabinose (Huang *et al.* 2016, 2017). The potential reaction pathways of monosaccharides (xylose, mannose, and galactose) by DFT calculations concluded that FF was more easily produced during the pyrolysis of xylose than the other products.

In contrast, during the pyrolysis of mannose and galactose, the formation of HMF was more favorable because of the higher energy of hydroxymethyl dissociation. The lower energy potential of the O-acetyl group readily broke to form acetic acid (Wang *et al.* 2013a). The pyrolysis pathway of xylobiose was investigated using the DFT method. The ring-opening reaction was the most kinetically favorable pathway, followed by the cleavage of the β -(1,4) glycosidic bond and the dehydration reaction (Li *et al.* 2017c). In recent years, with the development of computers, many complex and accurate models have been used for calculations. A hemicellulose model as glucomannan with O-acetyl groups and galactose side chains were more favorable for the glycosidic bond breakage and O-acetyl dissociation than xylan by DFT calculations (Wang *et al.* 2021b). The most favorable initial reaction was the cleavage of the 4-O-methylglucuronic acid unit. Furfural could be obtained from the ring-opening of 4-O-methylglucuronide by three different pathways, while O-methyl is mainly responsible for the generation of CH_3OH . In addition, the pathway for the generation of the special furan derivative 2-hydroxymethylene-tetrahydrofuran-3-one is verified for the first time by DFT calculations (Wu *et al.* 2019). The similar model (xylan containing multiple branched chains) for pyrolysis by DFT showed that during the initial pyrolysis of xylan, the branching broke easier than the depolymerization of the main chain, and the arabinose unit is more active than the 4-O-methylglucuronide unit (Hu *et al.* 2021a).

Lignin Pyrolysis Mechanism

M06-2X functional was used to study the pyrolysis process of PPE at the 6-31G* and 6-311++G** levels. The bond dissociation enthalpy (BDE) of β -O in PPE was 7.6 kcal/mol lower than that of C_{α} - C_{β} (Beste and Buchanan 2009). Similarly, BDE was calculated for four prevalent linkage bonds (β -O-4, α -O-4, β -5, and 5-5) in 69 lignin models. The results showed that C-C bonds were more stable than ether bonds, and β -O-4 linkage bonds were more persistent than other ether bonds (Kim *et al.* 2011). The pyrolytic behavior of a lignin dimer model (1-(4-hydroxy-3-methoxyphenyl)-2-(2-methoxyphenoxy)-1-ethanol) was analyzed by DFT and the main bond BDE order was C_{β} -O < C_{α} - C_{β} < C_{α} -OH < C_{α} - $C_{aromatic}$ < $C_{aromatic}$ -O. Nine possible radical reaction pathways were proposed, and the reaction energy barriers were calculated for each path (Shen *et al.* 2021). The vanillin pyrolysis process was simulated with DFT method at the M06-2X/6-31 G+(d,p) level. CO, benzene, catechol, phenol, and cyclopentadiene were the main products of the secondary pyrolysis of vanillin. Formyl, hydroxyl, and methoxy all contribute to the formation of CO (Wang *et al.* 2016).

CATALYTIC CONVERSION MECHANISM

Cellulose Catalytic Conversion Mechanism

The catalytic conversion of cellulose into high value-added chemicals and fuels is considered an effective way to utilize biomass energy. A novel cellulose conversion process using ILs as both solvent and catalyst has attracted much attention (Amarasekara and Owereh 2009; Jiang *et al.* 2011). [Bmim]Cl and [C₄SO₃Hmim]Cl were used as solvent and catalyst to study the conversion process of cellulose to glucose. The conversion included two basic steps: in the first step, the SO₃H group protonated the glycosidic oxygen and Cl⁻ attacked the anomeric carbon leading to the breakage of the glycosidic bond to form a glycosyl chloride intermediate. In the second step, the oxygen atom of the water molecule attacked the anomeric carbon, accompanying deprotonation of the SO₃⁻ group and C-Cl bond breakage so that the catalytic cycle of glycosidic bond hydrolysis is completed (Li *et al.* 2015a). In the presence of this IL, glucose was further converted to the platform chemical HMF. The DFT calculations revealed the existence of two possible pathways to facilitate the formation of HMF, and identified that 1,2-enediol is a necessary intermediate for both paths.

Dehydration is regarded as one of the important reactions in the catalytic conversion of cellulose. Six chemical reaction pathways were proposed to decompose glucose in supercritical water at the B3LYP/AGU-cc-pVDZ level. Water molecules play a role in transferring hydrogen atoms during dehydration and keto-enol rearrangement, which significantly reduces the potential barrier to the reaction (Zhang *et al.* 2016). The selective conversion from cellulose to platform chemicals, such as HMF (van Putten *et al.* 2013; Li *et al.* 2018), LaA (Holm *et al.* 2010; Castillo Martinez *et al.* 2013), and LA (Lin *et al.* 2012; Li *et al.* 2014), was a major challenge. The mechanism of the cellulose-catalyzed conversion process was elaborated at the molecular level through DFT simulations to help better understand and guide the experiments. Currently, the conversion of glucose to HMF was divided into two steps: glucose was first isomerized to fructose in the presence of catalysts, such as enzymes, Lewis acid, or bases, and then fructose was dehydrated under acidic conditions to produce HMF. Sn-BEA zeolites could isomerize glucose to fructose by O₂H deprotonation and hydrogen transfer from C₂ to C₁ to

isomerize acyclic glucose into deprotonated fructose intermediate (Yang *et al.* 2013). The introduction of SO₃H functional groups in ILs was a promising and versatile catalyst for the synthesis of HMF (Amarasekara and Owereh 2009). A series of Brønsted-Lewis acidic double cationic ILs could effectively convert glucose to HMF with a yield of up to 71% of HMF. The reaction mechanism is that AlCl₄⁻ facilitated the isomerization of glucose to fructose, while the SO₃H group could form hydrogen bonds with fructose to promote dehydration (Guo *et al.* 2020). In addition, sulfonated poly(phenylene sulfide) (SPPS) could convert glucose and cellulose directly to HMF in ILs. The SO₃H group of SPPS is both a proton donor (Brønsted acid) and a proton acceptor (conjugate base). The anions and cations of ILs in conjunction with SO₃H-SPPS helped stabilize the reaction intermediates and transition states, thus allowing easy conversion of glucose to HMF (Li *et al.* 2018).

The catalytic production of LaA from cellulose/glucose has been widely studied as a high-value platform chemical for producing fine chemicals and biodegradable plastics. Wang and co-workers elucidated the mechanism of conversion from cellulose to LaA from theoretical and experimental studies by adding Pb(II), including hydrolysis of cellulose to glucose, isomerization of glucose to fructose, cleavage of fructose to trisaccharide, and conversion of trisaccharide to LaA. The role of Pb(II) was to convert the main product of the reaction to LaA, and in the absence of Pb(II) fructose would be dehydrated to HMF (Wang *et al.* 2013b). Y(III) was used as a catalyst to selectively convert hemicellulose, and cellulose fractions to LaA with a LaA yield of 66.3%. [Y(OH)₂(H₂O)₂]⁺ significantly promoted the conversion of monosaccharides to LaA, especially facilitating the breakage of C3-C4 bonds of fructose. The visualization of the weak interactions (Fig. 7) showed that the initial intra- and interchain hydrogen bonds (blue part) in cellobiose were greatly weakened (green region) after the formation of new hydrogen bonds between H₃O⁺-Cl⁻ and cellobiose (Xu *et al.* 2020b). The catalytic system formed by MgO and D-LaA had a significantly synergistic effect on the chemical catalytic conversion of tricarbonic sugars to D-LaA. Quantum chemical calculations showed that [Mg(OH)(H₂O)₃]⁺, as the active substance, was mainly involved in the conversion of DHA to PA. Pre-added D-LaA, assisted by undissolved MgO, mainly promoted the enantioselective formation of D-LaA from PA conversion (Xu *et al.* 2021b).

The conversion of cellulose to LA was usually divided into three steps: hydrolysis of cellulose to glucose, conversion of glucose to HMF, and hydration of HMF to LA and formic acid. Cellulose could be selectively converted to LA in the IL of [C₃SO₃Hmim]HSO₄, and the specific conversion process from HMF to LA included (1) dehydration of C1 position and rehydration of C5 atom; (2) nucleophilic addition of water molecule to aldehyde group and protonation of C1 atom; (3) elimination of HCOOH, C4-C5 double bond electrophilic addition; and (4) ring-opening and subsequent enol-keto isomerization (Li *et al.* 2017a). A novel bifunctional catalyst, HScCl₄, with high selectivity and efficiency was developed for converting HMF to LA. The DFT results showed that the synergistic catalytic effect generated by the acidic sites of HScCl₄ significantly reduced the energy barriers of the reactants and intermediates, thus facilitating the conversion of HMF to LA (Liu *et al.* 2021a).

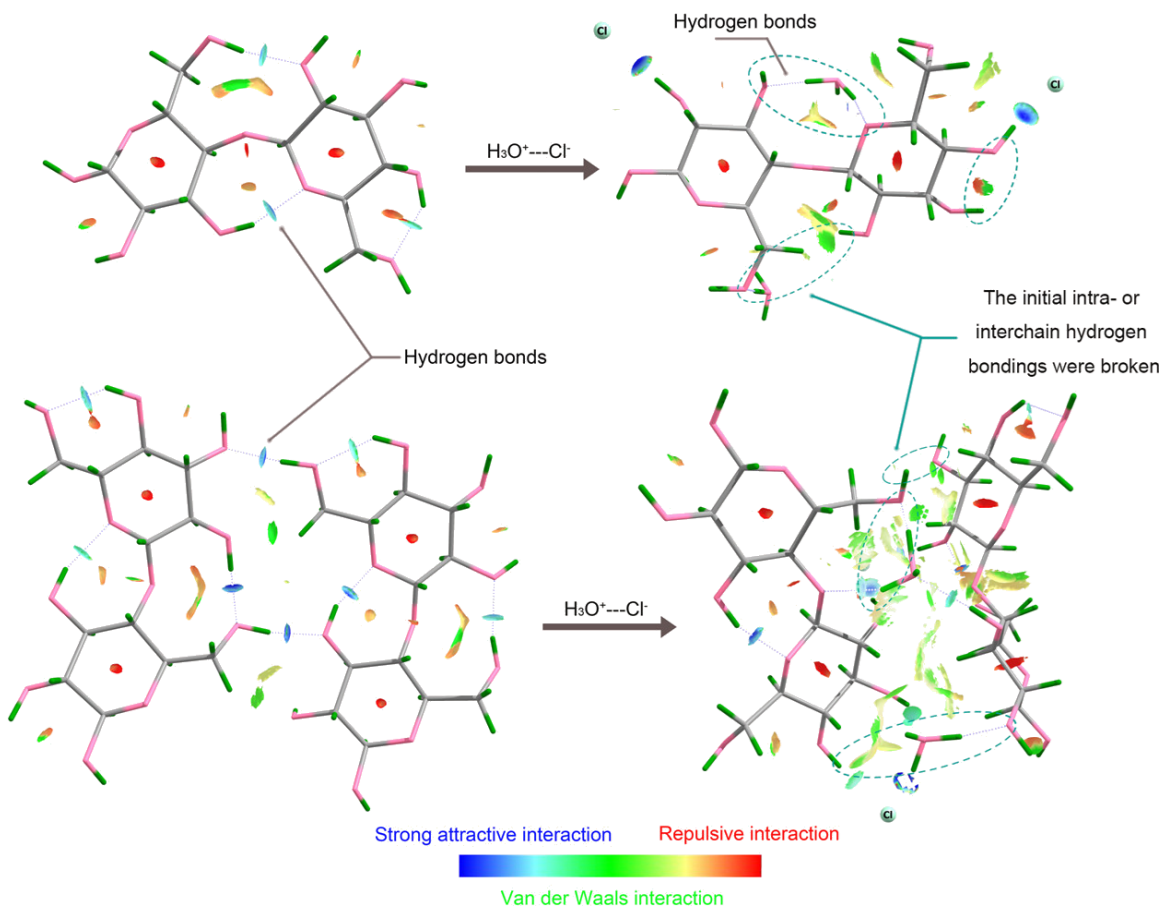


Fig. 7. The visualized weak interaction for the performance of $\text{H}_3\text{O}^+\text{-Cl}^-$ on the breaking of inter- and intrachain hydrogen bonds in cellobiose. Reprinted with permission from (Xu *et al.* 2020b). Copyright 2020 American Chemical Society.

Hemicellulose Catalytic Conversion Mechanism

Due to the structural similarity of hemicellulose and cellulose, the related chemicals converted from cellulose could also be converted by hemicellulose (Liu *et al.* 2009; Mäki-Arvela *et al.* 2011; Xing *et al.* 2011; Liu *et al.* 2012). FF was an important derivative in the decomposition of xylose, and the formation mechanism of xylose to FF was studied by Wang and co-workers using the DFT method. As an intermediate conversion of xylose to FF, xylulose had a low energy barrier, 163.6 kJ/mol in the gas phase and 150.8 kJ/mol in water. Adding water molecules could significantly reduce the reaction barriers to FF formation resulting in higher FF yields in the aqueous environment (Wang *et al.* 2015). A butanone-water mixture solvent was used for the acid-catalyzed conversion of xylose to FF. The MD simulations confirmed the competition between butanone and water molecules around xylose and FF. The appropriate amount of butanone could replace most water molecules around xylose and FF. Thus, it promoted the dehydration reaction of xylose and blocked the consumption of FF (Zhao *et al.* 2019). Some ILs could also be used as reaction media for hemicellulose conversion. Xylose could be converted to HMF and FF by acid catalysis in [Bmim]Cl (Sievers *et al.* 2009).

In addition, metal chlorides (CrCl_3 , $\text{CuCl}_2\cdot 2\text{H}_2\text{O}$, $\text{CrCl}_3/\text{LiCl}$, $\text{FeCl}_3\cdot 6\text{H}_2\text{O}$, LiCl , CuCl , and AlCl_3) and inorganic acids (H_2SO_4 , HCl , and H_3PO_4) were used as catalysts to catalyze the conversion of xylan to FF in [Bmim]Cl (Zhang *et al.* 2013). The $[\text{AlCl}_n]^{(n-3)-}$

not only weakened the glycosidic bond leading to the hydrolysis of xylan to xylose but also caused the isomerization of xylose to form enol and the dehydration to furfural (Zhang and Zhao 2010).

Although computer simulations are less studied in the catalytic conversion mechanism of hemicellulose, a portion of simulation studies exist for the conversion of hemicellulose-based FF to other value-added chemicals. Kojcinovic and co-workers studied the catalytic hydrogenation of furfural on MoO₂ and MoO₃ and suggested that the most abundant end product was isopropyl levulinate. The specific reaction pathway was the hydrogenation of furfural to produce furfuryl alcohol, followed by etherification to make isopropyl furfuryl ether, and finally isopropyl levulinate by ring-opening. The DFT results indicated stronger surface adsorption with directly exposed Mo atoms (Kojcinovic *et al.* 2021). The DFT calculations showed furfural was bound to the bimetallic surface mainly through C=O bonds, with the furan ring tilted away from the surface, leading to 2-methylfuran *via* the hydrodeoxygenation (HDO) reaction, and furfuryl alcohol was identified as a possible intermediate. Similar interactions of C=O groups with furan rings were confirmed on SiO₂-loaded FeNi bimetallic catalysts (Yu *et al.* 2014). In addition, the reaction pathways of furfural on Ni(111) monometallic and monolayer Fe/Ni(111) bimetallic surfaces were investigated. The DFT calculation showed that Fe/Ni(111) monolayer was an effective surface for furfural conversion and promoted the deoxygenation of furfural by extending the C=O bond of the carbonyl group (Yu and Chen 2015).

Lignin Catalytic Conversion Mechanism

Obtaining high value-added products from lignin was challenging due to the recalcitrant nature of the lignin structure. With the increasing scientific understanding of lignin and the application of novel catalysts, many new lignin degradation strategies have been proposed in combination with computer simulations (Mensah *et al.* 2022). The DFT was applied to explore the effect of H protons on the catalytic process of β -O-4 type lignin dimer, and showed that the breakage of the C _{β} -O bond was the main pathway for the cleavage of lignin macromolecules, and H protons weakened the C _{β} -O bond (Chen *et al.* 2021). The formic acid-catalyzed depolymerization of lignin models to monoaromatic compounds using DFT is shown in Fig. 8. The process included a formylation phase, an elimination phase, and a hydrolysis phase. Additionally, a new mechanism (E1H-3c4e) in the elimination phase was proposed, which had a lower potential barrier than the known E1 and E2 elimination (Qu *et al.* 2015).

The depolymerization of lignin was the essence of ILs as effective reagents for the biomass pretreatment process. [C₃SO₃HMIM][HSO₄] was used to catalyze the depolymerization of lignin to obtain low molecular weight products. The electron density could be transferred from the substrate to the electron-deficient imidazole ring as demonstrated by both experimental and DFT theoretical calculations. The formation of strong hydrogen bonds between the anion and the substrate played an essential role in the catalytic process (Singh *et al.* 2018). There was consensus that the anions in ILs could form hydrogen-bonding interactions with lignin, while the mechanism of cations in lignin depolymerization remains to be added. Due to the large number of computational studies employing ILs for catalytic degradation of lignin, the highlights of these simulation studies are summarized in Table 2.

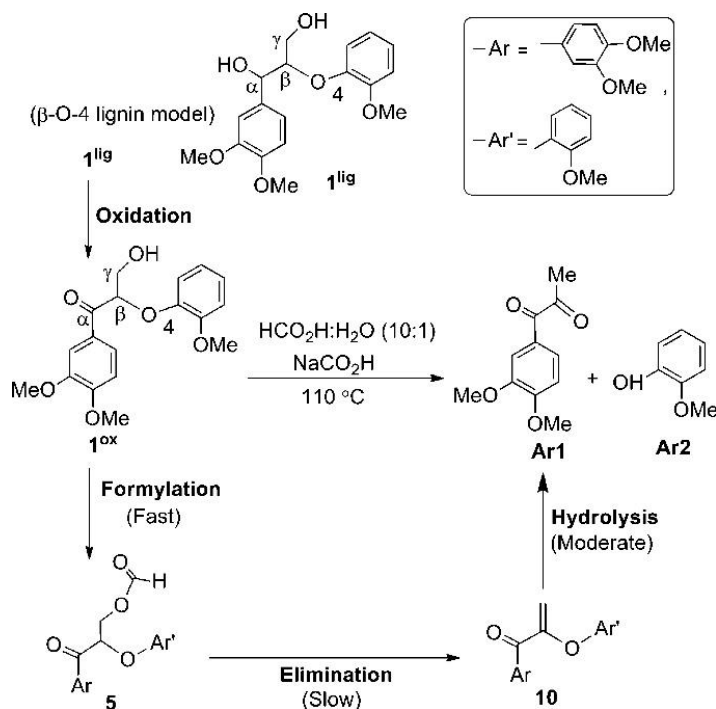


Fig. 8. Flow chart of model depolymerization of lignin to single aromatic compounds catalyzed by formic acid. Reprinted with permission from (Qu *et al.* 2015). Copyright 2015 American Chemical Society.

Table 2. Computational Study on Catalytic Degradation of Lignin by ILs

Lignin Models	ILs	Highlights	Ref.
VG	[Hmim]Cl	The catalytic processes of lignin model substances included dehydration and hydrolysis.	(Zhu <i>et al.</i> 2018)
GG	[C ₃ SO ₃ Hmim][HSO ₄]	Three possible cleavage routes for the β-O-4 bond: α-C-OH dehydration process, γ-C-OH dehydration process, and direct protonation process of the β-O bond.	(Zhang <i>et al.</i> 2019d)
VG	[C ₃ SO ₃ Hmim][HSO ₄]	Five stages of β-O-4 bond cleavage: proton dehydration process (bottleneck step), β-H elimination process, protonation process, hydroxylation step, and β-O-4 bond cleavage process.	(Jing <i>et al.</i> 2019)
PPC	[Bmim][FeCl ₄]	PPC broke through the γ-O ester bond to MPC.	(Zhang <i>et al.</i> 2019b)
HPE	[Hmim]Cl/AlCl ₃	Acid IL combined with AlCl ₃ exhibited higher catalytic activity for HPE.	(Janesko 2014)

Moreover, metals or metal oxides can also be involved in the lignin depolymerization process as catalysts. Copper particles loaded on γ -Al₂O₃ catalyzed the breakage of β-O-4 type lignin bonds under HDO conditions and produced large amounts of phenol and ethylbenzene (Strassberger *et al.* 2013). For Ru-catalyzed C-C bond breaking in lignin, a mechanism for C-C bond cleavage based on a trans-aldol reaction initiated by dehydrogenation was proposed based on experimental data and DFT calculations (vom Stein *et al.* 2015). The interaction and decomposition pathway of anisole on Pt(111) surface

was described in detail by Reocreux and co-workers and suggested that the key intermediate was the co-adsorption of phenoxy and methylene (Reocreux *et al.* 2016). The energy, geometry, and electronic structure of a lignin model (1,2-diphenylethanol) containing β -1 bonds was calculated by DFT on the (100) surface of different metals (Ni, Cu, and W). The presence of hydrogen significantly changed the adsorption morphology, stability, and bond dissociation energy of the C-C bonds of the model compounds. The amount of hydrogen coverage did not affect adsorption on the W surface. The Ni surface preferentially interacted with the aromatic ring, while the Cu surface could cleave the C-C bonds without breaking the aromatic ring (Cheng *et al.* 2018).

Based on monometallic catalysts, researchers added some nonmetals to achieve higher efficiency of lignin-catalyzed depolymerization. For example, the doping of cyclic carbene in Ni as a catalyst was applied to the catalytic reaction of aryl ethers. The DFT calculations showed that the coordination of excess base ($t\text{BuO}^-$) could promote the rate-determining C-O activation process, leading to the dissociation of ArO^- ligand (Xu *et al.* 2016). The selective cleavage of β -O-4, β -1, and C-C bonds catalyzed by copper and alkali solutions to produce high yields of aromatic acids and phenol was first reported by Hu and co-workers. The DFT calculations showed that the oxidation of β -O-4 ketone to peroxide intermediates by Cu and O_2 reduced the dissociation energy of the $\text{C}_\alpha\text{-C}_\beta$ bond (Hu *et al.* 2021b). The mechanism of HDO reaction was investigated during the decomposition of anisole over a bifunctional catalyst consisting of metal and Brønsted acid using DFT. For the adsorption of anisole, the adsorption energies of Co, Mo, Ni, and Cu were higher than those of other transition metals, and the Ni and Mo metal sites were good promoters of the HDO reaction (Zhang *et al.* 2018). The catalytic pathway for the cleavage of BPE in the liquid phase with Ni-based and zeolite-based catalysts was explored by He and co-workers. In the presence of Ni/SiO₂, selective hydrogenolysis was mainly used to break the $\text{C}_{\text{aliphatic}}\text{-O}$ bond. The protonation of BPE was the initial reaction path for the aqueous phase. Radical reactions in non-polar solvents led to the primary benzyl and phenoxy groups in undecane, leading to heavier condensation products as long as metals were absent to provide dissociated hydrogen (He *et al.* 2014).

Furthermore, Table 3 provides an exhaustive list of relevant simulation studies of multicomponent catalysts in the field of lignin-catalyzed depolymerization. These catalysts included at least two metal-based substances, *e.g.*, bimetallic catalysts, alloy catalysts, metal-metal oxide catalysts, and metal-metal organic framework catalysts. Table 3 also has more recent and relatively emerging methods for electrocatalytic lignin cracking.

Table 3. Simulation of Polymetallic Catalysts in Lignin Catalyzing and Depolymerization

Lignin Models	Catalytic Systems	Highlights	Ref.
PPE BPE DPE	IRMOF-74(n)-Mg	IRMOF-74(III)-Mg had the highest catalytic rate, and the Mg-O bond weakened the substrate ether bond and increased the lifetime in the open metal site.	Stavila <i>et al.</i> 2019
Anisole	HZSM-5 zeolite-loaded bimetallic catalyst (Ni-Mo, Ni-Fe, and Mo-Fe)	The strong binding of phenolic compounds to the bimetallic surface of Ni-Mo-based catalysts led to higher yields of benzene, toluene, and xylene from the	Zhang <i>et al.</i> 2019a

		decomposition of anisole deoxygenation reactions.	
Guaiacol	Pd/Al ₂ O ₃ catalyst + hydrogen carrier	Compared to saturated donors, unsaturated donors could rehydrogenate, thus competing with guaiacol and reducing the effective H transfer rate.	Fraga <i>et al.</i> 2020
BPE	Pd nanoparticles + Ce-BTC (MOF)	Pd/Ce-BTC had higher activity than Pd/CeO ₂ due to 1) higher Pd ⁰ /Pd ²⁺ ratio on Pd/Ce-BTC, 2) higher BPE adsorption on Pd/Ce-BTC, and 3) higher phenol adsorption on Pd/CeO ₂ .	Kar <i>et al.</i> 2020
Guaiacol	RuNi/SiO ₂ -ZrO ₂ RuCo/SiO ₂ -ZrO ₂	Ru-Ni and Ru-Co bimetallic catalysts showed a high capacity for hydrogen and guaiacol adsorption, and guaiacol activation (electron transfer). RuCo catalysts were more effective than RuNi catalysts for HDO reaction of lignin oil.	Li <i>et al.</i> 2020; Shu <i>et al.</i> 2020
PC	TT-Nb ₂ O ₅ Ru/TiO ₂ Ru/TiO ₂ Ru/Al ₂ O ₃	The C _{aromatic} -C cleavage process of PC on phosphoric acid deposited TT-Nb ₂ O ₅ (100), TiO ₂ (101), ZrO ₂ (-111), and γ-Al ₂ O ₃ (110) and were investigated by the DFT method.	Dong <i>et al.</i> 2021
Phenol Anisole	M@Pt(211) (M = Co, Fe, Mo) monoatomic alloy	The deoxygenation or partially catalyzed HDO process on M@Pt(211) was more efficient than the original Pt(211).	Liu and An 2021
Vanillin	NiCo@N-CNTs/CMF	The outstanding HDO catalytic performance of the catalyst was attributed to the selective adsorption and activation of C=O greatly promoted by the synergistic effect of alloyed Ni-Co nanoparticles.	Wang <i>et al.</i> 2021a
2-PE	PtRu electrode + electrocatalytic oxidation method	The substrate electrolysis process was strongly restricted, the C-C cleavage was strongly hindered, and the adsorption of reaction intermediates and products led to strong deactivation of the anode catalyst.	Beliaeva <i>et al.</i> 2020
2-P-1-PE	Pt ₁ /N-CNTs + electrocatalytic oxidation method	The atomically dispersed Pt-N ₃ C ₁ site on Pt ₁ /N-CNTs was highly active and selective for the C _α -C _β bond breaking in the β-O-4 model.	Cui <i>et al.</i> 2021

CONCLUSION AND PERSPECTIVES

The utilization of biomass resources as a renewable resource has long been of increasing interest, and most research focused on techniques related to dissolution, pyrolysis, and catalytic conversion processes. The successful application of computer simulations, including quantum chemical calculations and molecular dynamics simulations, could provide a wealth of information on the precise reaction energies and complex intramolecular interactions between lignocellulosic components that were not experimentally achievable. The development of simulation methods facilitated the development of technologies for the utilization of lignocellulosic biomass materials and have become a powerful approach to explaining the mechanisms behind the utilization of lignocellulose. Several questions regarding the microscopic mechanisms should be clarified in the following work.

Precise and reasonable models are important, especially for hemicellulose and lignin. Due to the complex structure of lignin, in the current models with monomers, dimers, or short-chain polymers, DFT methods are applied rather than MD to calculate lignin systems. The development of accurate lignin models and with the help of experimental data enabled researchers to understand better the structure of lignin, the interactions between lignin and the environment and solvents, the reasons why lignin was in the folded or unfolded state, and the pathways and products of lignin degradation and pyrolysis. In contrast, its simulation studies were fewer for hemicellulose, usually as an adjunct to cellulose conversion studies, which is detrimental to understanding the structural properties of hemicellulose and its role in the plant cell wall.

DFT is uniquely positioned as a major simulation tool for finding transition states, determining reaction paths, predicting products, and among many lignocellulosic biomass conversion processes. Because DFT can not simulate the behavior of large systems, the classical MD force field for lignocellulosic materials (CHARMM, GROMOS, and GLACAM 06) does not describe lignocellulosic biomass conversion processes well, the ReaxFF force field for reaction processes is in the preliminary stage of development, the development and refinement of reaction force fields has played a key role in promoting the development of technologies for utilizing lignocellulosic biomass materials.

Computer simulations can be used as a complementary description of experimental phenomena and as a prediction of experimental phenomena when they are not possible or practical. They will play a key role in lignocellulosic biomass conversion technology.

ACKNOWLEDGMENTS

This work was supported by the National Natural Science Foundation of China (22078114), the National Key Research and Development Program (2021YFE0104500), Key Research and Development Program of Guangzhou Science and Technology Program (202103000011), and the Natural Science Foundation of Guangdong Province (2021A1515010360).

REFERENCES CITED

- Agarwal, V., Dauenhauer, P. J., Huber, G. W., and Auerbach, S. M. (2012). “Ab initio dynamics of cellulose pyrolysis: Nascent decomposition pathways at 327 and 600 °C,” *Journal of the American Chemical Society* 134(36), 14958-14972. DOI: 10.1021/ja305135u
- Amarasekara, A. S., and Owereh, O. S. (2009). “Hydrolysis and decomposition of cellulose in Brønsted acidic ionic liquids under mild conditions,” *Industrial & Engineering Chemistry Research* 48(22), 10152-10155. DOI: 10.1021/ie901047u
- Andanson, J.-M., Bordes, E., Devémy, J., Leroux, F., Pádua, A. A. H., and Gomes, M. F. C. (2014). “Understanding the role of co-solvents in the dissolution of cellulose in ionic liquids,” *Green Chemistry* 16(5), 2528-2538. DOI: 10.1039/C3GC42244E
- Beliaeva, K., Elsheref, M., Walden, D., Dappozze, F., Nieto-Marquez, A., Gil, S., Guillard, C., Vernoux, P., Steinmann, S. N., and Caravaca, A. (2020). “Towards understanding lignin electrolysis: Electro-oxidation of a beta-O-4 linkage model on PtRu electrodes,” *Journal of the Electrochemical Society* 167, Article ID 134511. DOI: 10.1149/1945-7111/abb8b5
- Bergensträhle, M., Wohler, J., Himmel, M. E., and Brady, J. W. (2010). “Simulation studies of the insolubility of cellulose,” *Carbohydrate Research* 345(14), 2060-2066. DOI: 10.1016/j.carres.2010.06.017
- Beste, A., and Buchanan, A. C. (2009). “Computational study of bond dissociation enthalpies for lignin model compounds. substituent effects in phenethyl phenyl ethers,” *The Journal of Organic Chemistry* 74(7), 2837-2841. DOI: 10.1021/jo9001307
- Brooks, B. R., Bruccoleri, R. E., Olafson, B. D., States, D. J., Swaminathan, S., and Karplus, M. (1983). “CHARMM: A program for macromolecular energy, minimization, and dynamics calculations,” *Journal of Computational Chemistry* 4(2), 187-217. DOI: 10.1002/jcc.540040211
- Buehler, M. J., and Ackbarow, T. (2007). “Fracture mechanics of protein materials,” *Materials Today* 10(9), 46-58. DOI: 10.1016/S1369-7021(07)70208-0
- Caldeweyher, E., Bannwarth, C., and Grimme, S. (2017). “Extension of the D3 dispersion coefficient model,” *The Journal of Chemical Physics* 147(3), Article ID 034112. DOI: 10.1063/1.4993215
- Castillo Martinez, F. A., Balciunas, E. M., Salgado, J. M., Domínguez González, J. M., Converti, A., and Oliveira, R. P. d. S. (2013). “Lactic acid properties, applications and production: A review,” *Trends in Food Science & Technology* 30(1), 70-83. DOI: 10.1016/j.tifs.2012.11.007
- Chen, M., Zhong, W. P., Wu, K., Wei, G., Hu, Z. H., Zheng, W. G., Ruan, H. F., Zhang, H. Y., and Xiao, R. (2021). “Catalytic pyrolysis mechanism of beta-O-4 type of lignin dimer: The role of H proton,” *Energy & Fuels* 35(1), 575-582. DOI: 10.1021/acs.energyfuels.0c03588
- Cheng, C. B., Shen, D. K., and Gu, S. (2018). “Adsorption of C-C linkage-contained lignin model compound over the metal surface of catalysts: Quantum simulation,” *Topics in Catalysis* 61(15), 1783-1791. DOI: 10.1007/s11244-018-1013-3
- Cui, T. T., Ma, L. N., Wang, S. B., Ye, C. L., Liang, X., Zhang, Z. D., Meng, G., Zheng, L. R., Hu, H. S., Zhang, J. W., *et al.* (2021). “Atomically dispersed Pt-N3C1 sites enabling efficient and selective electrocatalytic C-C bond cleavage in lignin models

- under ambient conditions,” *Journal of the American Chemical Society* 143(25), 9429-9439. DOI: 10.1021/jacs.1c02328
- Damm, W., Frontera, A., Tirado-Rives, J., and Jorgensen, W. L. (1997). “OPLS all-atom force field for carbohydrates,” *Journal of Computational Chemistry* 18(16), 1955-1970. DOI: 10.1002/(SICI)1096-987X(199712)18:16<1955::AID-JCC1>3.0.CO;2-L
- Dong, K., Liu, X., Dong, H., Zhang, X., and Zhang, S. (2017). “Multiscale studies on ionic liquids,” *Chemical Reviews* 117(10), 6636-6695. DOI: 10.1021/acs.chemrev.6b00776
- Dong, L., Xia, J., Guo, Y., Liu, X. H., Wang, H. F., and Wang, Y. Q. (2021). “Mechanisms of C-aromatic-C bonds cleavage in lignin over NbOx-supported Ru catalyst,” *Journal of Catalysis* 394, 94-103. DOI: 10.1016/j.jcat.2021.01.001
- Feofilova, E. P., and Mysyakina, I. S. (2016). “Lignin: Chemical structure, biodegradation, and practical application (a review),” *Applied Biochemistry and Microbiology* 52(6), 573-581. DOI: 10.1134/S0003683816060053
- Fraga, G., Yin, Y. L., Konarova, M., Hasan, M. D., Laycock, B., Yuan, Q. H., Batalha, N., and Pratt, S. (2020). “Hydrocarbon hydrogen carriers for catalytic transfer hydrogenation of guaiacol,” *International Journal of Hydrogen Energy* 45(51), 27381-27391. DOI: 10.1016/j.ijhydene.2020.07.136
- Garcia Calvo-Flores, F., and Dobado, J. A. (2010). “Lignin as renewable raw material,” *Chemosuschem* 3(11), 1227-1235. DOI: 10.1002/cssc.201000157
- Gibson, L. J. (2012). “The hierarchical structure and mechanics of plant materials,” *Journal of The Royal Society Interface* 9(76), 2749-2766. DOI: 10.1098/rsif.2012.0341
- Girio, F. M., Fonseca, C., Carvalheiro, F., Duarte, L. C., Marques, S., and Bogel-Lukasik, R. (2010). “Hemicelluloses for fuel ethanol: A review,” *Bioresource Technology* 101(13), 4775-4800. DOI: 10.1016/j.biortech.2010.01.088
- Goerigk, L., and Grimme, S. (2011). “A thorough benchmark of density functional methods for general main group thermochemistry, kinetics, and noncovalent interactions,” *Physical Chemistry Chemical Physics* 13(14), 6670-6688. DOI: 10.1039/C0CP02984J
- Grimme, S. (2004). “Accurate description of van der Waals complexes by density functional theory including empirical corrections,” *Journal of Computational Chemistry* 25(12), 1463-1473. DOI: 10.1002/jcc.20078
- Grimme, S. (2006). “Semiempirical GGA-type density functional constructed with a long-range dispersion correction,” *Journal of Computational Chemistry* 27(15), 1787-1799. DOI: 10.1002/jcc.20495
- Grimme, S., Antony, J., Ehrlich, S., and Krieg, H. (2010). “A consistent and accurate ab initio parametrization of density functional dispersion correction (DFT-D) for the 94 elements H-Pu,” *The Journal of Chemical Physics* 132(15), Article ID 154104. DOI: 10.1063/1.3382344
- Grimme, S. (2011). “Density functional theory with London dispersion corrections,” *WIREs Computational Molecular Science* 1(2), 211-228. DOI: 10.1002/wcms.30
- Gross, A. S., Bell, A. T., and Chu, J.-W. (2013). “Preferential interactions between lithium chloride and glucan chains in N,N-dimethylacetamide drive cellulose dissolution,” *The Journal of Physical Chemistry B* 117(12), 3280-3286. DOI: 10.1021/jp311770u

- Gross, A. S., Bell, A. T., and Chu, J.-W. (2011). "Thermodynamics of cellulose solvation in water and the ionic liquid 1-butyl-3-methylimidazolium chloride," *The Journal of Physical Chemistry B* 115(46), 13433-13440. DOI: 10.1021/jp202415v
- Guo, J., Zhang, D., Duan, C., and Liu, C. (2010). "Probing anion–cellulose interactions in imidazolium-based room temperature ionic liquids: a density functional study," *Carbohydrate Research* 345(15), 2201-2205. DOI: 10.1016/j.carres.2010.07.036
- Guo, W., Zuo, M., Zhao, J., Li, C., Xu, Q., Xu, C., Wu, H., Sun, Z., and Chu, W. (2020). "Novel Brønsted–Lewis acidic di-cationic ionic liquid for efficient conversion carbohydrate to platform compound," *Cellulose* 27(12), 6897-6908. DOI: 10.1007/s10570-020-03275-7
- Gupta, K. M., Hu, Z., and Jiang, J. (2013). "Molecular insight into cellulose regeneration from a cellulose/ionic liquid mixture: effects of water concentration and temperature," *RSC Advances* 3(13), 4425-4433. DOI: 10.1039/C3RA22561E
- He, J. Y., Lu, L., Zhao, C., Mei, D. H., and Lercher, J. A. (2014). "Mechanisms of catalytic cleavage of benzyl phenyl ether in aqueous and apolar phases," *Journal of Catalysis* 311, 41-51. DOI: 10.1016/j.jcat.2013.10.024
- Hermans, J., Berendsen, H. J. C., Van Gunsteren, W. F., and Postma, J. P. M. (1984). "A consistent empirical potential for water–protein interactions," *Biopolymers* 23(8), 1513-1518. DOI: 10.1002/bip.360230807
- Hohenberg, P. C., and Kohn, W. (1964). "Inhomogeneous electron gas," *Physical Review* 136(3B), B864-B871. DOI: 10.1103/PhysRev.136.B864
- Holm, M. S., Saravanamurugan, S., and Taarning, E. (2010). "Conversion of sugars to lactic acid derivatives using heterogeneous zeotype catalysts," *Science* 328(5978), 602-605. DOI: 10.1126/science.1183990
- Hu, B., Xie, W. L., Li, H., Li, K., Lu, Q., and Yang, Y. P. (2021a). "On the mechanism of xylan pyrolysis by combined experimental and computational approaches," *Proceedings of the Combustion Institute* 38(3), 4215-4223. DOI: 10.1016/j.proci.2020.06.172
- Hu, Y. Z., Yan, L., Zhao, X. L., Wang, C. U., Li, S., Zhang, X. H., Ma, L. L., and Zhang, Q. (2021b). "Mild selective oxidative cleavage of lignin C-C bonds over a copper catalyst in water," *Green Chemistry* 23(18), 7030-7040. DOI: 10.1039/d1gc02102h
- Huang, X., Cheng, D., Chen, F., and Zhan, X. (2013). "Reaction pathways of β -d-glucopyranose pyrolysis to syngas in hydrogen plasma: A density functional theory study," *Bioresource Technology* 143, 447-454. DOI: 10.1016/j.biortech.2013.06.019
- Huang, J. B., He, C., Wu, L. Q., and Tong, H. (2017). "Theoretical studies on thermal decomposition mechanism of arabinofuranose," *Journal of the Energy Institute* 90(3), 372-381. DOI: 10.1016/j.joei.2016.04.005
- Huang, J. B., He, C., Wu, L. Q., and Tong, H. (2016). "Thermal degradation reaction mechanism of xylose: A DFT study," *Chemical Physics Letters* 658, 114-124. DOI: 10.1016/j.cplett.2016.06.025
- Huo, F., Liu, Z., and Wang, W. (2013). "Cosolvent or antisolvent? A molecular view of the interface between ionic liquids and cellulose upon addition of another molecular solvent," *The Journal of Physical Chemistry B* 117(39), 11780-11792. DOI: 10.1021/jp407480b
- Janesko, B. G. (2014). "Acid-catalyzed hydrolysis of lignin β -O-4 linkages in ionic liquid solvents: A computational mechanistic study," *Physical Chemistry Chemical Physics* 16(11), 5423-5433. DOI: 10.1039/C3CP53836B

- Janesko, B. G. (2011). "Modeling interactions between lignocellulose and ionic liquids using DFT-D," *Physical Chemistry Chemical Physics* 13(23), 11393-11401. DOI: 10.1039/C1CP20072K
- Jiang, F., Zhu, Q., Ma, D., Liu, X., and Han, X. (2011). "Direct conversion and NMR observation of cellulose to glucose and 5-hydroxymethylfurfural (HMF) catalyzed by the acidic ionic liquids," *Journal of Molecular Catalysis A: Chemical* 334(1), 8-12. DOI: 10.1016/j.molcata.2010.10.006
- Jing, Y. R., Mu, X. L., Han, Z., Liu, C. B., and Zhang, D. J. (2019). "Mechanistic insight into beta-O-4 linkage cleavage of lignin model compound catalyzed by a SO₃H-functionalized imidazolium ionic liquid: An unconventional E1 elimination," *Molecular Catalysis* 463, 140-149. DOI: 10.1016/j.mcat.2018.12.002
- Ju, Z. Y., Yu, Y. H., Feng, S. K., Lei, T. Y., Zheng, M. J., Ding, L. Y., and Yu, M. T. (2022). "Theoretical mechanism on the cellulose regeneration from a cellulose/emimOAc mixture in anti-solvents," *Materials* 15(3), Article ID 1158. DOI: 10.3390/ma15031158
- Jung, G. S., Wang, S., Qin, Z., Martin-Martinez, F. J., Warner, J. H., and Buehler, M. J. (2018). "Interlocking friction governs the mechanical fracture of bilayer MoS₂," *ACS Nano* 12(4), 3600-3608. DOI: 10.1021/acsnano.8b00712
- Jung, G. S., Wang, S., Qin, Z., Zhou, S., Danaie, M., Kirkland, A. I., Buehler, M. J., and Warner, J. H. (2019). "Anisotropic fracture dynamics due to local lattice distortions," *ACS Nano* 13(5), 5693-5702. DOI: 10.1021/acsnano.9b01071
- Kadokawa, R., Endo, T., Yasaka, Y., Ninomiya, K., Takahashi, K., and Kuroda, K. (2021). "Cellulose preferentially dissolved over xylan in ionic liquids through precise anion interaction regulated by bulky cations," *ACS Sustainable Chemistry & Engineering* 9(26), 8686-8691. DOI: 10.1021/acssuschemeng.1c02492
- Kar, A. K., Kaur, S. P., Kumar, T. J. D., and Srivastava, R. (2020). "Efficient hydrogenolysis of aryl ethers over Ce-MOF supported Pd NPs under mild conditions: Mechanistic insight using density functional theoretical calculations," *Catalysis Science & Technology* 10(20), 6892-6901. DOI: 10.1039/d0cy01279c
- Kim, M.-C., Sim, E., and Burke, K. (2013). "Understanding and reducing errors in density functional calculations," *Physical Review Letters* 111(7), Article ID 073003. DOI: 10.1103/PhysRevLett.111.073003
- Kim, S., Chmely, S. C., Nimlos, M. R., Bomble, Y. J., Foust, T. D., Paton, R. S., and Beckham, G. T. (2011). "Computational study of bond dissociation enthalpies for a large range of native and modified lignins," *The Journal of Physical Chemistry Letters* 2(22), 2846-2852. DOI: 10.1021/jz201182w
- Kirschner, K. N., Yongye, A. B., Tschampel, S. M., González-Outeiriño, J., Daniels, C. R., Foley, B. L., and Woods, R. J. (2008). "GLYCAM06: A generalizable biomolecular force field. Carbohydrates," *J Comput Chem* 29(4), 622-655. DOI: 10.1002/jcc.20820
- Kohn, W., and Sham, L. J. (1965). "Self-consistent equations including exchange and correlation effects," *Physical Review* 140(4A), A1133-A1138. DOI: 10.1103/10.1103/physrev.140.a1133
- Kojcinovic, A., Kovacic, Z., Hus, M., Likozar, B., and Grilc, M. (2021). "Furfural hydrogenation, hydrodeoxygenation and etherification over MoO₂ and MoO₃: A combined experimental and theoretical study," *Applied Surface Science* 543, Article ID 114836. DOI: 10.1016/j.apsusc.2020.148836

- Lancefield, C. S., and Westwood, N. J. (2015). "The synthesis and analysis of advanced lignin model polymers," *Green Chemistry* 17(11), 4980-4990. DOI: 10.1039/c5gc01334h
- Li, J., Jiang, Z., Hu, L., and Hu, C. (2014). "Selective conversion of cellulose in corncob residue to levulinic acid in an aluminum trichloride–sodium chloride system," *Chemsuschem* 7(9), 2482-2488. DOI: 10.1002/cssc.201402384
- Li, J., Li, J., Zhang, D., and Liu, C. (2015a). "Theoretical explanation for how SO₃H-functionalized ionic liquids promote the conversion of cellulose to glucose," *ChemPhysChem* 16(14), 3044-3048. DOI: 10.1002/cphc.201500424
- Li, Y., Liu, X., Zhang, S., Yao, Y., Yao, X., Xu, J., and Lu, X. (2015b). "Dissolving process of a cellulose bunch in ionic liquids: A molecular dynamics study," *Physical Chemistry Chemical Physics* 17(27), 17894-17905. DOI: 10.1039/C5CP02009C
- Li, J. J., Jing, Y. R., Liu, C. B., and Zhang, D. J. (2017a). "A theoretical elucidation: Why does a SO₃H-functionalized imidazolium-based ionic liquid catalyze the conversion of 5-hydroxymethylfurfural to levulinic acid?," *New Journal of Chemistry* 41(17), 8714-8720. DOI: 10.1039/c7nj00878c
- Li, Y., Liu, X., Zhang, Y., Jiang, K., Wang, J., and Zhang, S. (2017b). "Why only ionic liquids with unsaturated heterocyclic cations can dissolve cellulose: A simulation study," *ACS Sustainable Chemistry & Engineering* 5(4), 3417-3428. DOI: 10.1021/acssuschemeng.7b00073
- Li, Z. Y., Liu, C., Xu, X. X., and Li, Q. B. (2017c). "A theoretical study on the mechanism of xylobiose during pyrolysis process," *Computational and Theoretical Chemistry* 1117, 130-140. DOI: 10.1016/j.comptc.2017.08.014
- Li, Z., Su, K., Ren, J., Yang, D., Cheng, B., Kim, C. K., and Yao, X. (2018). "Direct catalytic conversion of glucose and cellulose," *Green Chemistry* 20(4), 863-872. DOI: 10.1039/C7GC03318D
- Li, R. X., Qiu, J. J., Chen, H. Q., Shu, R. Y., Chen, Y., Liu, Y., and Liu, P. F. (2020). "Hydrodeoxygenation of phenolic compounds and raw lignin-oil over bimetallic RuNi catalyst: An experimental and modeling study focusing on adsorption properties," *Fuel* 281, Article ID 118758. DOI: 10.1016/j.fuel.2020.118758
- Lin, H., Strull, J., Liu, Y., Karmiol, Z., Plank, K., Miller, G., Guo, Z., and Yang, L. (2012). "High yield production of levulinic acid by catalytic partial oxidation of cellulose in aqueous media," *Energy & Environmental Science* 5(12), 9773-9777. DOI: 10.1039/C2EE23225A
- Liu, Z. W., Remsing, R. C., Moore, P. B., and Moyna, G. (2007). "Molecular dynamics study of the mechanism of cellulose dissolution in the ionic liquid 1-n-butyl-3-methylimidazolium chloride," in: *Ionic Liquids IV*, Vol. 975, American Chemical Society, Washington, D.C., USA, pp. 335-350.
- Liu, L., Sun, J., Cai, C., Wang, S., Pei, H., and Zhang, J. (2009). "Corn stover pretreatment by inorganic salts and its effects on hemicellulose and cellulose degradation," *Bioresource Technology* 100(23), 5865-5871. DOI: 10.1016/j.biortech.2009.06.048
- Liu, Z., Ma, C., Gao, C., and Xu, P. (2012). "Efficient utilization of hemicellulose hydrolysate for propionic acid production using *Propionibacterium acidipropionici*," *Bioresource Technology* 114, 711-714. DOI: 10.1016/j.biortech.2012.02.118
- Liu, G., Sun, H., Liu, G., Zhang, H., Yuan, S., and Zhu, Q. (2018). "A molecular dynamics study of cellulose inclusion complexes in NaOH/urea aqueous solution," *Carbohydrate Polymers* 185, 12-18. DOI: 10.1016/j.carbpol.2017.12.055

- Liu, R. R., and An, W. (2021). “Stepped M@Pt(211) (M = Co, Fe, Mo) single-atom alloys promote the deoxygenation of lignin-derived phenolics: Mechanism, kinetics, and descriptors,” *Catalysis Science & Technology* 11(21), 7047-7059. DOI: 10.1039/d1cy01258d
- Liu, S. W., Cheng, X. L., Sun, S. Q., Chen, Y. G., Bian, B., Liu, Y., Tong, L., Yu, H. L., Ni, Y. H., and Yu, S. T. (2021a). “High-yield and high-efficiency conversion of HMF to levulinic acid in a green and facile catalytic process by a dual-function Bronsted-Lewis acid HScCl₄ catalyst,” *ACS Omega* 6(24), 15940-15947. DOI: 10.1021/acsomega.1c01607
- Liu, Z., Ku, X., Jin, H., and Yang, S. (2021b). “Research on the microscopic reaction mechanism of cellulose pyrolysis using the molecular dynamics simulation,” *Journal of Analytical and Applied Pyrolysis* 159, Article ID 105333. DOI: 10.1016/j.jaap.2021.105333
- Lu, B., Xu, A., and Wang, J. (2014). “Cation does matter: How cationic structure affects the dissolution of cellulose in ionic liquids,” *Green Chemistry* 16(3), 1326-1335. DOI: 10.1039/C3GC41733F
- Mäki-Arvela, P., Salmi, T., Holmbom, B., Willför, S., and Murzin, D. Y. (2011). “Synthesis of sugars by hydrolysis of hemicelluloses- A review,” *Chemical Reviews* 111(9), 5638-5666. DOI: 10.1021/cr2000042
- Malaspina, D. C., and Faraudo, J. (2019). “Molecular insight into the wetting behavior and amphiphilic character of cellulose nanocrystals,” *Advances in Colloid and Interface Science* 267, 15-25. DOI: 10.1016/j.cis.2019.02.003
- Manna, B., Datta, S., and Ghosh, A. (2021). “Understanding the dissolution of softwood lignin in ionic liquid and water mixed solvents,” *International Journal of Biological Macromolecules* 182, 402-412. DOI: 10.1016/j.ijbiomac.2021.04.006
- Mazeau, K., and Rivet, A. (2008). “Wetting the (110) and (100) surfaces of Iβ cellulose studied by molecular dynamics,” *Biomacromolecules* 9(4), 1352-1354. DOI: 10.1021/bm7013872
- Meng, X., Devemy, J., Verney, V., Gautier, A., Husson, P., and Andanson, J. M. (2017). “Improving cellulose dissolution in ionic liquids by tuning the size of the ions: Impact of the length of the alkyl chains in tetraalkylammonium carboxylate,” *Chemsuschem* 10(8), 1749-1760. DOI: 10.1002/cssc.201601830
- Mensah, M., Tia, R., Adei, E., and de Leeuw, N. H. (2022). “A DFT mechanistic study on base-catalyzed cleavage of the beta-O-4 ether linkage in lignin: Implications for selective lignin depolymerization,” *Frontiers in Chemistry* 10, Article ID 793759. DOI: 10.3389/fchem.2022.793759
- Miyamoto, H., Schnupf, U., Ueda, K., and Yamane, C. (2015). “Dissolution mechanism of cellulose in a solution of aqueous sodium hydroxide revealed by molecular dynamics simulations,” *Nordic Pulp & Paper Research Journal* 30(1), 67-77. DOI: 10.3183/npprj-2015-30-01-p067-077
- Mohan, M., Viswanath, P., Banerjee, T., and Goud, V. V. (2018). “Multiscale modelling strategies and experimental insights for the solvation of cellulose and hemicellulose in ionic liquids,” *Molecular Physics* 116(15-16), 2108-2128. DOI: 10.1080/00268976.2018.1447152
- Mood, S. H., Golfeshan, A. H., Tabatabaei, M., Jouzani, G. S., Najafi, G., Gholami, M., and Ardjmand, M. (2013). “Lignocellulosic biomass to bioethanol, a comprehensive review with a focus on pretreatment,” *Renewable & Sustainable Energy Reviews* 27, 77-93. DOI: 10.1016/j.rser.2013.06.033

- Moyer, P., Smith, M. D., Abdoulmoumine, N., Chmely, S. C., Smith, J. C., Petridis, L., and Labbe, N. (2018). "Relationship between lignocellulosic biomass dissolution and physicochemical properties of ionic liquids composed of 3-methylimidazolium cations and carboxylate anions," *Physical Chemistry Chemical Physics* 20(4), 2508-2516. DOI: 10.1039/c7cp07195g
- Murillo, J. D., Moffet, M., Biernacki, J. J., and Northrup, S. (2015). "High-temperature molecular dynamics simulation of cellobiose and maltose," *AIChE Journal* 61(8), 2562-2570. DOI: 10.1002/aic.14854
- Oostenbrink, C., Villa, A., Mark, A. E., and Van Gunsteren, W. F. (2004). "A biomolecular force field based on the free enthalpy of hydration and solvation: The GROMOS force-field parameter sets 53A5 and 53A6," *Journal of Computational Chemistry* 25(13), 1656-1676. DOI: 10.1002/jcc.20090
- O'Sullivan, A. C. (1997). "Cellulose: The structure slowly unravels," *Cellulose* 4(3), 173-207. DOI: 10.1023/A:1018431705579
- Payal, R. S., Bharath, R., Periyasamy, G., and Balasubramanian, S. (2012). "Density functional theory investigations on the structure and dissolution mechanisms for cellobiose and xylan in an ionic liquid: Gas phase and cluster calculations," *The Journal of Physical Chemistry B* 116(2), 833-840. DOI: 10.1021/jp207989w
- Petridis, L., Schulz, R., and Smith, J. C. (2011). "Simulation analysis of the temperature dependence of lignin structure and dynamics," *Journal of the American Chemical Society* 133(50), 20277-20287. DOI: 10.1021/ja206839u
- Qi, S.-C., Hayashi, J.-i., and Zhang, L. (2016). "Recent application of calculations of metal complexes based on density functional theory," *RSC Advances* 6(81), 77375-77395. DOI: 10.1039/C6RA16168E
- Qu, S. L., Dang, Y. F., Song, C. Y., Guo, J. D., and Wang, Z. X. (2015). "Depolymerization of oxidized lignin catalyzed by formic acid exploits an unconventional elimination mechanism involving 3c-4e bonding: A DFT mechanistic study," *ACS Catalysis* 5(11), 6386-6396. DOI: 10.1021/acscatal.5b01095
- Rabideau, B. D., and Ismail, A. E. (2015). "Effect of water content in N-methylmorpholine N-oxide/cellulose solutions on thermodynamics, structure, and hydrogen bonding," *The Journal of Physical Chemistry B* 119(48), 15014-15022. DOI: 10.1021/acs.jpcc.5b07500
- Ralph, J., Lapierre, C., and Boerjan, W. (2019). "Lignin structure and its engineering," *Current Opinion in Biotechnology* 56, 240-249. DOI: 10.1016/j.copbio.2019.02.019
- Reocreux, R., Hamou, C. A. O., Michel, C., Giorgi, J. B., and Sautet, P. (2016). "Decomposition mechanism of anisole on Pt(111): Combining single-crystal experiments and first-principles calculations," *ACS Catalysis* 6(12), 8166-8178. DOI: 10.1021/acscatal.6b02253
- Rivas, S., Vila, C., Santos, V., and Carlos Parajo, J. (2016). "Furfural production from birch hemicelluloses by two-step processing: a potential technology for biorefineries," *Holzforschung* 70(10), 901-910. DOI: 10.1515/hf-2015-0255
- Sangha, A. K., Petridis, L., Smith, J. C., Ziebell, A., and Parks, J. M. (2012). "Molecular simulation as a tool for studying lignin," *Environmental Progress & Sustainable Energy* 31(1), 47-54. DOI: 10.1002/ep.10628
- Shen, Q., Fu, Z., Li, R., and Wu, Y. (2021). "A study on the pyrolysis mechanism of a β -O-4 lignin dimer model compound using DFT combined with Py-GC/MS," *Journal of Thermal Analysis and Calorimetry* 146(4), 1751-1761. DOI: 10.1007/s10973-020-10130-1

- Shi, J., Balamurugan, K., Parthasarathi, R., Sathitsuksanoh, N., Zhang, S., Stavila, V., Subramanian, V., Simmons, B. A., and Singh, S. (2014). "Understanding the role of water during ionic liquid pretreatment of lignocellulose: Co-solvent or anti-solvent?," *Green Chemistry* 16(8), 3830-3840. DOI: 10.1039/C4GC00373J
- Shu, R. Y., Li, R. X., Liu, Y., Wang, C., Liu, P. F., and Chen, Y. (2020). "Enhanced adsorption properties of bimetallic RuCo catalyst for the hydrodeoxygenation of phenolic compounds and raw lignin-oil," *Chemical Engineering Science* 227, Article ID 115920. DOI: 10.1016/j.ces.2020.115920
- Si, T., Huang, K., Lin, Y., and Gu, M. (2019). "ReaxFF study on the effect of CaO on cellulose pyrolysis," *Energy & Fuels* 33(11), 11067-11077. DOI: 10.1021/acs.energyfuels.9b02583
- Sievers, C., Musin, I., Marzioletti, T., Valenzuela Olarte, M. B., Agrawal, P. K., and Jones, C. W. (2009). "Acid-catalyzed conversion of sugars and furfurals in an ionic-liquid phase," *Chemsuschem* 2(7), 665-671. DOI: 10.1002/cssc.200900092
- Singh, S. K., Banerjee, S., Vanka, K., and Dhepe, P. L. (2018). "Understanding interactions between lignin and ionic liquids with experimental and theoretical studies during catalytic depolymerisation," *Catalysis Today* 309, 98-108. DOI: 10.1016/j.cattod.2017.09.050
- Stavila, V., Foster, M., Brown, J. W., Davis, R. W., Edgington, J., Benin, A. I., Zarkesh, R. A., Parthasarathi, R., Hoyt, D. W., Walter, E. D., *et al.* (2019). "IRMOF-74(n)-Mg: A novel catalyst series for hydrogen activation and hydrogenolysis of C-O bonds," *Chemical Science* 10(42), 9880-9892. DOI: 10.1039/c9sc01018a
- Strassberger, Z., Alberts, A. H., Louwse, M. J., Tanase, S., and Rothenberg, G. (2013). "Catalytic cleavage of lignin beta-O-4 link mimics using copper on alumina and magnesia-alumina," *Green Chemistry* 15(3), 768-774. DOI: 10.1039/c3gc37056a
- Terrett, O. M., and Dupree, P. (2019). "Covalent interactions between lignin and hemicelluloses in plant secondary cell walls," *Current Opinion in Biotechnology* 56, 97-104. DOI: 10.1016/j.copbio.2018.10.010
- Thomas, L. H. (1927). "The calculation of atomic fields," *Mathematical Proceedings of the Cambridge Philosophical Society* 23(5), 542-548. DOI: 10.1017/S0305004100011683
- van Duin, A. C. T., Dasgupta, S., Lorant, F., and Goddard, W. A. (2001). "ReaxFF: A reactive force field for hydrocarbons," *The Journal of Physical Chemistry A* 105(41), 9396-9409. DOI: 10.1021/jp004368u
- van Putten, R.-J., van der Waal, J. C., de Jong, E., Rasrendra, C. B., Heeres, H. J., and de Vries, J. G. (2013). "Hydroxymethylfurfural, a versatile platform chemical made from renewable resources," *Chemical Reviews* 113(3), 1499-1597. DOI: 10.1021/cr300182k
- Velioglu, S., Yao, X., Devémy, J., Ahunbay, M. G., Tantekin-Ersolmaz, S. B., Dequidt, A., Costa Gomes, M. F., and Pádua, A. A. H. (2014). "Solvation of a cellulose microfibril in imidazolium acetate ionic liquids: Effect of a cosolvent," *The Journal of Physical Chemistry B* 118(51), 14860-14869. DOI: 10.1021/jp508113a
- vom Stein, T., den Hartog, T., Buendia, J., Stoychev, S., Mottweiler, J., Bolm, C., Klankermayer, J., and Leitner, W. (2015). "Ruthenium-catalyzed C-C bond cleavage in lignin model substrates," *Angewandte Chemie-International Edition* 54(20), 5859-5863. DOI: 10.1002/anie.201410620

- Vu, T., Chaffee, A., and Yarovsky, I. (2002). "Investigation of lignin-water interactions by molecular simulation," *Molecular Simulation* 28(10-11), 981-991. DOI: 10.1080/089270204000002610
- Wang, S. R., Ru, B., Lin, H. Z., and Luo, Z. Y. (2013a). "Degradation mechanism of monosaccharides and xylan under pyrolytic conditions with theoretic modeling on the energy profiles," *Bioresource Technology* 143, 378-383. DOI: 10.1016/j.biortech.2013.06.026
- Wang, Y., Deng, W., Wang, B., Zhang, Q., Wan, X., Tang, Z., Wang, Y., Zhu, C., Cao, Z., Wang, G., *et al.* (2013b). "Chemical synthesis of lactic acid from cellulose catalysed by lead(II) ions in water," *Nature Communications* 4(1), Article ID 2141. DOI: 10.1038/ncomms3141
- Wang, M., Liu, C., Li, Q. B., and Xu, X. X. (2015). "Theoretical insight into the conversion of xylose to furfural in the gas phase and water," *Journal of Molecular Modeling* 21(11), Article ID 296. DOI: 10.1007/s00894-015-2843-6
- Wang, M., Liu, C., Xu, X., and Li, Q. (2016). "Theoretical study of the pyrolysis of vanillin as a model of secondary lignin pyrolysis," *Chemical Physics Letters* 654, 41-45. DOI: 10.1016/j.cplett.2016.03.058
- Wang, Y., Liu, L., Chen, P., Zhang, L., and Lu, A. (2018). "Cationic hydrophobicity promotes dissolution of cellulose in aqueous basic solution by freezing–thawing," *Physical Chemistry Chemical Physics* 20(20), 14223-14233. DOI: 10.1039/C8CP01268G
- Wang, J., Qian, Y., Li, L., and Qiu, X. (2020). "Atomic force microscopy and molecular dynamics simulations for study of lignin solution self-assembly mechanisms in organic–aqueous solvent mixtures," *Chemsuschem* 13(17), 4420-4427. DOI: 10.1002/cssc.201903132
- Wang, D. D., Gong, W. B., Zhang, J. F., Han, M. M., Chen, C., Zhang, Y. X., Wang, G. Z., Zhang, H. M., and Zhao, H. J. (2021a). "Encapsulated Ni-Co alloy nanoparticles as efficient catalyst for hydrodeoxygenation of biomass derivatives in water," *Chinese Journal of Catalysis* 42(11), 2027-2037. DOI: 10.1016/S1872-2067(21)63828-7
- Wang, G. Y., Dai, G. X., Ding, S. Q., Wu, J. F., and Wang, S. R. (2021b). "A new insight into pyrolysis mechanism of three typical actual biomass: The influence of structural differences on pyrolysis process," *Journal of Analytical and Applied Pyrolysis* 156, Article ID 105184. DOI: 10.1016/j.jaap.2021.105184
- Wang, Y., Li, Y., Zhang, C., Yang, L., Fan, X., and Chu, L. (2021c). "A study on co-pyrolysis mechanisms of biomass and polyethylene via ReaxFF molecular dynamic simulation and density functional theory," *Process Safety and Environmental Protection* 150, 22-35. DOI: 10.1016/j.psep.2021.04.002
- Wernersson, E., Stenqvist, B., and Lund, M. (2015). "The mechanism of cellulose solubilization by urea studied by molecular simulation," *Cellulose* 22(2), 991-1001. DOI: 10.1007/s10570-015-0548-8
- Wu, J., Liu, C., and Li, Q. B. (2019). "Thermal decomposition mechanism of O-acetyl-4-O-methylglucurono-xylan," *Journal of Molecular Modeling* 25(8), Article ID 234. DOI: 10.1007/s00894-019-4117-1
- Xing, R., Qi, W., and Huber, G. W. (2011). "Production of furfural and carboxylic acids from waste aqueous hemicellulose solutions from the pulp and paper and cellulosic ethanol industries," *Energy & Environmental Science* 4(6), 2193-2205. DOI: 10.1039/C1EE01022K

- Xu, L. P., Chung, L. W., and Wu, Y. D. (2016). "Mechanism of Ni-NHC catalyzed hydrogenolysis of aryl ethers: Roles of the excess base," *ACS Catalysis* 6(1), 483-493. DOI: 10.1021/acscatal.5b02089
- Xu, H., Che, X., Ding, Y., Kong, Y., Li, B., and Tian, W. (2019). "Effect of crystallinity on pretreatment and enzymatic hydrolysis of lignocellulosic biomass based on multivariate analysis," *Bioresource Technology* 279, 271-280. DOI: 10.1016/j.biortech.2018.12.096
- Xu, H., Peng, J. P., Kong, Y., Liu, Y., Su, Z. N., Li, B., Song, X. M., Liu, S. W., and Tian, W. D. (2020). "Key process parameters for deep eutectic solvents pretreatment of lignocellulosic biomass materials: A review," *Bioresource Technology* 310, Article ID 123416. DOI: 10.1016/j.biortech.2020.123416
- Xu, H., Kong, Y., Peng, J., Wang, W., and Li, B. (2021a). "Mechanism of deep eutectic solvent delignification: Insights from molecular dynamics simulations," *ACS Sustainable Chemistry & Engineering* 9(20), 7101-7111. DOI: 10.1021/acssuschemeng.1c01260
- Xu, S. G., He, T., Li, J. M., Huang, Z. M., and Hu, C. W. (2021b). "Enantioselective synthesis of D-lactic acid via chemocatalysis using MgO: Experimental and molecular-based rationalization of the triose's reactivity and preliminary insights with raw biomass," *Applied Catalysis B-Environmental* 292, Article ID 120145. DOI: 10.1016/j.apcatb.2021.120145
- Yang, G., Pidko, E. A., and Hensen, E. J. M. (2013). "The mechanism of glucose isomerization to fructose over Sn-BEA zeolite: A periodic density functional theory study," *Chemsuschem* 6(9), 1688-1696. DOI: 10.1002/cssc.201300342
- Yang, X. X., Fu, Z. W., Han, D. D., Zhao, Y. Y., Li, R., and Wu, Y. L. (2020). "Unveiling the pyrolysis mechanisms of cellulose: Experimental and theoretical studies," *Renewable Energy* 147, 1120-1130. DOI: 10.1016/j.renene.2019.09.069
- Yao, Y., Li, Y., Liu, X., Zhang, X., Wang, J., Yao, X., and Zhang, S. (2015). "Mechanistic study on the cellulose dissolution in ionic liquids by density functional theory," *Chinese Journal of Chemical Engineering* 23(11), 1894-1906. DOI: 10.1016/j.cjche.2015.07.018
- Yu, W. T., and Chen, J. G. G. (2015). "Reaction pathways of model compounds of biomass-derived oxygenates on Fe/Ni bimetallic surfaces," *Surface Science* 640, 159-164. DOI: 10.1016/j.susc.2015.01.009
- Yu, W. T., Xiong, K., Ji, N., Porosoff, M. D., and Chen, J. G. G. (2014). "Theoretical and experimental studies of the adsorption geometry and reaction pathways of furfural over FeNi bimetallic model surfaces and supported catalysts," *Journal of Catalysis* 317, 253-262. DOI: 10.1016/j.jcat.2014.06.025
- Yuan, X., and Cheng, G. (2015). "From cellulose fibrils to single chains: Understanding cellulose dissolution in ionic liquids," *Physical Chemistry Chemical Physics* 17(47), 31592-31607. DOI: 10.1039/C5CP05744B
- Yui, T., and Hayashi, S. (2007). "Molecular dynamics simulations of solvated crystal models of cellulose Ia and III," *Biomacromolecules* 8(3), 817-824. DOI: 10.1021/bm060867a
- Zakzeski, J., Bruijninx, P. C. A., Jongerius, A. L., and Weckhuysen, B. M. (2010). "The catalytic valorization of lignin for the production of renewable chemicals," *Chemical Reviews* 110(6), 3552-3599. DOI: 10.1021/cr900354u

- Zhang, Z., and Zhao, Z. K. (2010). "Microwave-assisted conversion of lignocellulosic biomass into furans in ionic liquid," *Bioresource Technology* 101(3), 1111-1114. DOI: 10.1016/j.biortech.2009.09.010
- Zhang, L., Yu, H., Wang, P., Dong, H., and Peng, X. (2013). "Conversion of xylan, d-xylose and lignocellulosic biomass into furfural using AlCl₃ as catalyst in ionic liquid," *Bioresource Technology* 130, 110-116. DOI: 10.1016/j.biortech.2012.12.018
- Zhang, Y., Liu, C., and Chen, X. (2016). "Mechanism of glucose conversion in supercritical water by DFT study," *Journal of Analytical and Applied Pyrolysis* 119, 199-207. DOI: 10.1016/j.jaap.2016.02.018
- Zhang, J. J., Fidalgo, B., Shen, D. K., Zhang, X. L., and Gu, S. (2018). "Mechanism of hydrodeoxygenation (HDO) in anisole decomposition over metal loaded Bronsted acid sites: Density functional theory (DFT) study," *Molecular Catalysis* 454, 30-37. DOI: 10.1016/j.mcat.2018.05.015
- Zhang, J. J., Fidalgo, B., Wagland, S., Shen, D. K., Zhang, X. L., and Gu, S. (2019a). "Deoxygenation in anisole decomposition over bimetallic catalysts supported on HZSM-5," *Fuel* 238, 257-266. DOI: 10.1016/j.fuel.2018.10.129
- Zhang, T., Zhang, Y. Q., Wang, Y. L., Huo, F., Li, Z. M., Zang, Q., He, H. Y., and Li, X. H. (2019b). "Theoretical insights into the depolymerization mechanism of lignin to methyl p-hydroxycinnamate by [Bmim][FeCl₄] ionic liquid," *Frontiers in Chemistry* 7, Article ID 446. DOI: 10.3389/fchem.2019.00446
- Zhang, Y. Q., He, H. Y., Liu, Y. R., Wang, Y. L., Huo, F., Fan, M. H., Adidharma, H., Li, X. H., and Zhang, S. J. (2019c). "Recent progress in theoretical and computational studies on the utilization of lignocellulosic materials," *Green Chemistry* 21(1), 9-35. DOI: 10.1039/c8gc02059k
- Zhang, Y. Q., Huo, F., Wang, Y. L., Xia, Y., Tan, X., Zhang, S. J., and He, H. Y. (2019d). "Theoretical elucidation of beta-O-4 bond cleavage of lignin model compound promoted by sulfonic acid-functionalized ionic liquid," *Frontiers in Chemistry* 7, Article ID 78. DOI: 10.3389/fchem.2019.00078
- Zhao, Y., Liu, X., Wang, J., and Zhang, S. (2013). "Effects of anionic structure on the dissolution of cellulose in ionic liquids revealed by molecular simulation," *Carbohydrate Polymers* 94(2), 723-730. DOI: 10.1016/j.carbpol.2013.02.011
- Zhao, Y., Xu, H., Wang, K., Lu, K., Qu, Y., Zhu, L., and Wang, S. (2019). "Enhanced furfural production from biomass and its derived carbohydrates in the renewable butanone-water solvent system," *Sustainable Energy & Fuels* 3(11), 3208-3218. DOI: 10.1039/C9SE00459A
- Zhou, S., Weimer, P. J., Hatfield, R. D., Runge, T. M., and Digman, M. (2014). "Improving ethanol production from alfalfa stems via ambient-temperature acid pretreatment and washing," *Bioresource Technology* 170, 286-292. DOI: 10.1016/j.biortech.2014.08.002
- Zhou, S., Yang, Q., and Runge, T. M. (2015). "Ambient-temperature sulfuric acid pretreatment to alter structure and improve enzymatic digestibility of alfalfa stems," *Industrial Crops and Products* 70, 410-416. DOI: 10.1016/j.indcrop.2015.03.068
- Zhou, S. F., Jin, K., and Buehler, M. J. (2021). "Understanding plant biomass via computational modeling," *Advanced Materials* 33(28), Article ID 2003206. DOI: 10.1002/adma.202003206
- Zhu, Y., Yan, J., Liu, C., and Zhang, D. (2017). "Modeling interactions between a β -O-4 type lignin model compound and 1-allyl-3-methylimidazolium chloride ionic liquid," *Biopolymers* 107(8), Article ID e23022. DOI: 10.1002/bip.23022

Zhu, Y. T., Han, Z., Fu, L. J., Liu, C. B., and Zhang, D. J. (2018). “Cleavage of the β -O-4 bond in a lignin model compound using the acidic ionic liquid 1-H-3-methylimidazolium chloride as catalyst: A DFT mechanistic study,” *Journal of Molecular Modeling* 24(11), Article ID 322. DOI: 10.1007/s00894-018-3854-x

Article submitted: June 17, 2022; Peer review completed: August 6, 2022; Revised version received and accepted: August 23, 2022; Published: August 30, 2022.
DOI: 10.15376/biores.17.4.Kong